


 Cite this: *RSC Adv.*, 2024, 14, 26400

# A comprehensive review of production, applications, and the path to a sustainable energy future with hydrogen

 Abdulrahman bin Jumah 

Green hydrogen, a versatile and sustainable energy carrier, has garnered increasing attention as a critical element in the global transition to a low-carbon economy. This review article comprehensively examines the production, applications, and potential of green hydrogen, accompanied by the challenges and future prospects associated with its widespread adoption. The production of green hydrogen is a central focus, due to its environmental benefits and distinctive characteristics. The article delves into the various techniques and technologies employed in green hydrogen production, emphasizing the need for cost reduction and increased scale for economic viability. Focusing particularly on applications, the review discusses the diverse sectors where green hydrogen demonstrates immense promise. Challenges and limitations are explored, including the intermittent nature of renewable energy sources, high production costs, and the need for extensive hydrogen infrastructure. The article also highlights the pressing need for innovation in electrolysis technology and materials, emphasizing the potential for cost reduction and increased efficiency. As industries gradually transition to green hydrogen as a cleaner feedstock, its demand and cost-competitiveness are projected to increase. This review article thoroughly evaluates the current status of green hydrogen and provides valuable insights into its potential role in the transition to a sustainable energy system.

 Received 21st June 2024  
 Accepted 4th August 2024

DOI: 10.1039/d4ra04559a

[rsc.li/rsc-advances](https://rsc.li/rsc-advances)

## 1. Introduction

Energy plays a pivotal role in numerous everyday functions, encompassing transportation, mobility, culinary activities, water purification, communication, and more.<sup>1,2</sup> Our planet is confronted with two significant dilemmas – environmental pollution and an energy crisis, both of which have been intensified by the swift progression of human civilization.<sup>3,4</sup> The growing use of fossil fuels to satisfy our current energy requirements has raised concerns about an impending energy crisis. This, in turn, has sparked a renewed enthusiasm for advancing renewable alternatives to address the increasing energy demands of the developing world.<sup>5,6</sup> The overreliance on fossil fuels has induced global warming through carbon dioxide emissions, underscoring the urgent need for the enthusiastic encouragement of clean and renewable energy sources.<sup>7</sup> In 2019, the annual global carbon dioxide emissions resulting from energy sources amounted to 33.3 metric gigatons, and this growth rate is projected to cause a significant rise in Earth's temperature by several degrees unless effective mitigation measures are implemented.<sup>8</sup> Nowadays, an increasing number of nations are declaring their shift towards greener energy sources and more environmentally conscious forms of

transportation. This phenomenon, often denoted to as the “worldwide energy transition” is gaining substantial momentum at a rapid pace.<sup>9,10</sup> Some of these major transitions' projects can be found in Table 1.

Taking proactive measures against climate change, as indicated by the International Energy Agency (IEA) study, could bring about \$26 trillion in economic benefits and 65 million new jobs by 2030.<sup>20</sup> Hence, renewable energy sources are increasingly gaining traction to achieve environmentally friendly and sustainable energy systems. This is due to their non-carbon, widespread availability, and high-energy-density characteristics.<sup>21–23</sup> Broadly speaking, the utilization of renewable energy stands as the most appealing approach, holding the potential to substantially reduce or even eliminate the reliance on fossil fuels. Renewable energy sources have experienced a significant increase in generation and adoption over the past decade. Some of these sources are even harnessed for large-scale electricity production, as seen in the case of solar energy,<sup>24,25</sup> wind energy,<sup>26–28</sup> biomass energy,<sup>29,30</sup> and ocean energy.<sup>31,32</sup>

Hydrogen (H<sub>2</sub>), a gas that is both colorless and odorless, possesses remarkable flammability. Several sources, such as biomass, natural gas, and water, can be used to obtain hydrogen, which is the lightest and most abundant element in the universe.<sup>33–35</sup> Utilizing H<sub>2</sub> as a fuel source involves the transformation of this gas into electricity within a hydrogen fuel

Chemical Engineering Department, College of Engineering, King Saud University, P.O. Box 800, Riyadh 11421, Saudi Arabia. E-mail: [abinjumah@ksu.edu.sa](mailto:abinjumah@ksu.edu.sa)



Table 1 Illustrations of some of the most extensive renewable energy endeavors employing various technologies across the globe

Type	Name	Country	Power capacity (MW)	Year	Ref.
Biomass power plant	Alholmens Kraft power plant	Finland	240	2002	11
Hydroelectric power	Three Gorges dam	China	22 500	2003	12
On-shore wind farm	Gansu wind farm	China	7965	2009	13
Biomass power plant	Ironbridge power plant	United Kingdom	740	2012	14
Biomass power plant	Polaniec biomass power plant	Poland	220	2012	15
Photovoltaics & hydroelectric power	Longyangxia dam solar park	China	2130	2015	16
Parabolic trough and solar power tower (CSP)	Ouarzazate solar power station	Morocco	580	2016	17
Photovoltaics	Bhadla solar park	India	2245	2018	18
Photovoltaics	Huanghe hydropower hainan solar park	China	2200	2020	19

cell (FC). These cells are distinguished by their exceptional efficiency, boasting rates of up to 60%. Moreover, they demonstrate an environmentally friendly character, as they generate no detrimental emissions, yielding only water and heat as by-products.<sup>36,37</sup> H<sub>2</sub> stands as an eco-friendly fuel, emitting no environmentally harmful molecules during combustion or oxidation at lower temperatures.<sup>38,39</sup> H<sub>2</sub> shows significant potential for reducing carbon emissions in the energy sector and achieving net-zero production by 2050. Driven by these compelling attributes of hydrogen, several nations have just unveiled plans and initiatives aimed at establishing sustainable, renewable (green) hydrogen ecosystems.<sup>40–42</sup>

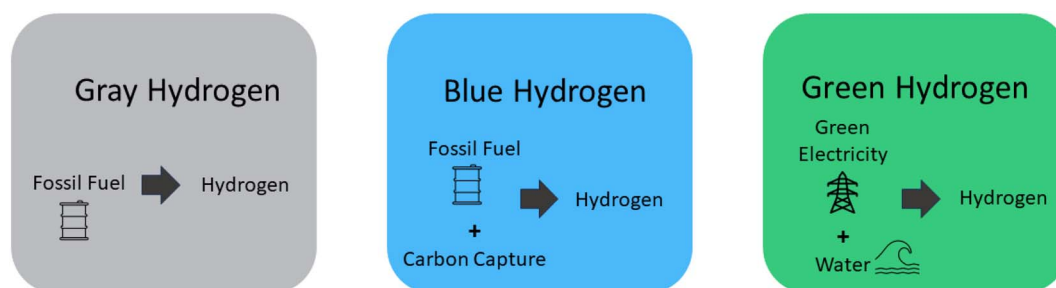
H<sub>2</sub> can be generated from both sustainable and non-sustainable origins, resulting in the categorizations of green, blue, and gray hydrogen.<sup>43</sup> These types and their origins are shown in brief in (Fig. 1).

The production of H<sub>2</sub> through the utilization of fossil fuels is classified as gray H<sub>2</sub>, denoting its association with environmental consequences and carbon emissions resulting from the combustion of these finite resources.<sup>44</sup> The majority of present-day H<sub>2</sub> production stems from fossil fuels incorporating no carbon dioxide capture. While this stands as the most direct approach to hydrogen generation, its sustainability is questionable.<sup>45</sup> Gray H<sub>2</sub> is acquired through processes that yield greenhouse gas emissions exceeding 36.4 grams of carbon dioxide per megajoule (MJ), regardless of whether these processes rely on renewable or non-renewable resources.<sup>46,47</sup> In the current landscape, the foremost origins of the H<sub>2</sub> supply can be attributed to the exploitation of coal and natural gas. The

industrial utilization of H<sub>2</sub> spans across the globe; however, the act of producing H<sub>2</sub> presents a notable concern due to the substantial carbon dioxide emissions it contributes annually. This interplay underscores the delicate balance between the practical applications of H<sub>2</sub> and the environmental ramifications inherent in its generation.<sup>48,49</sup> In summary, the production of gray H<sub>2</sub> from fossil fuels carries significant environmental implications and carbon emissions. While fossil fuels dominate current H<sub>2</sub> production, their sustainability remains uncertain.

The outcome of this process is blue H<sub>2</sub>, which emerges from the utilization of fossil fuels in combination with methods involving carbon utilization, storage, and absorption.<sup>50,51</sup> Blue H<sub>2</sub> is commonly synthesized from natural gas, frequently employing steam reforming techniques coupled with carbon capture and storage. While certain approaches to blue H<sub>2</sub> production involve carbon absorption, it's important to note that this method doesn't inherently eliminate carbon emissions.<sup>52</sup> Producing a substantial quantity of blue H<sub>2</sub> could play a vital role in supporting the expanding worldwide and local H<sub>2</sub> supply chains and their associated fuels. The highest projected efficiency for carbon dioxide absorption stands between 85% to 95%, resulting in a leakage of around 5% to 15% of the total carbon.<sup>53</sup>

H<sub>2</sub> derived from sustainable and renewable resources is classified as green H<sub>2</sub>, signifying its origin through environmentally friendly methods that harness sources like solar, wind, or hydropower.<sup>54–56</sup> An increasingly prominent technique within this sector, garnering noteworthy focus in recent times, is the electrolytic generation of H<sub>2</sub>.<sup>57</sup> The production of green H<sub>2</sub> using

Fig. 1 Types of H<sub>2</sub> and their origin.

renewable energy sources is expected to increase rapidly in the near future. Multiple ongoing and forthcoming initiatives are aligned with this trajectory.<sup>58,59</sup> Nonetheless, achieving substantial cost reduction necessitates increased mass production, dedicated research, and comprehensive development efforts. In accordance with this pattern, the scope of projects has experienced exponential expansion in recent times. H<sub>2</sub> generated from renewable sources has the hypothetical to greatly enhance renewable energy output. It is currently technically viable and has the imminent potential to become a prominent global economic contender.<sup>60</sup> Anticipations from experts indicate that, by 2050, the cost of green H<sub>2</sub> will probably fall to a level below \$1 per kilogram, thus rendering green H<sub>2</sub> a more competitive option. This underscores the pressing requirement for persistent research and development efforts in the realm of H<sub>2</sub> energy. Such investments are essential because H<sub>2</sub> is forecasted to emerge as the preferred choice for fuel in the forthcoming years, primarily due to its substantial energy content and environmentally advantageous attributes.<sup>61</sup>

## 2. Production methods

Despite its prevalence in the universe, H<sub>2</sub> is mostly found in combination with other elements on Earth. Thus, the production of H<sub>2</sub> hinges on its extraction from various compounds. H<sub>2</sub> can be produced from various sources, containing sustainable resources like biomass and water, as well as non-renewable sources such as crude oil, coal, and natural gas. Although fossil fuels are a cheap way to produce H<sub>2</sub>, concerns about their limited reserves and environmental impact have steered the search for alternative methods.

Some of the already used methods, such as pyrolysis, have several advantages, including the production of H<sub>2</sub>-rich fuel, rapid and efficient decomposition of feedstock, and great flexibility. However, there are also certain disadvantages, such as the high energy requirements and the potential for tar formation. Gasification offers several advantages, including the capability to convert a wide range of feedstocks, extraordinary productivity, and the potential to generate value-added products alongside H<sub>2</sub> production. Nevertheless, there are also some disadvantages, such as electrode deactivation, substantial energy requirements, and the necessity for exceptionally durable equipment. Reforming offers several advantages, including a high capacity to reform diverse materials, cost-effective construction, rapid response capabilities, and compactness. However, there are also some drawbacks, such as high energy requirements, a significant reduction in electrode lifetime, and the need for catalyst regeneration. The data included in Table 2.

### 2.1. Steam methane reforming

Steam methane reforming (SMR) (Fig. 2) is the most widely used technique for producing H<sub>2</sub> from natural gas.<sup>72</sup> In a typical SMR process, steam is combined with natural gas and methane-rich gases (like those from landfills and biogas) using a catalyst to construct hydrogen and carbon monoxide ( $\text{CH}_4 + \text{H}_2\text{O} \rightarrow \text{CO} +$

$3\text{H}_2$ ). Typically, SMR yields a H<sub>2</sub>-rich gas composition, containing approximately 70% to 75% H<sub>2</sub> by dry mass, along with small quantities of carbon dioxide, carbon monoxide, and methane. Reforming natural gas accounts for about 50% of the global H<sub>2</sub> supply currently.<sup>73</sup> Nonetheless, given that natural gas is consumed directly and results in the production of CO<sub>2</sub>, this method raises significant environmental concerns.<sup>74</sup> A much greener approach is imperative for the future.

### 2.2. Plasma

The introduction of innovative technologies, such as plasma, within thermochemical conversion methods, offers new avenues for the cost-effective production of H<sub>2</sub>, accompanied by the creation of value-added products. Plasma is categorized into two main types: non-thermal and thermal plasma, distinguished by their characteristics, including energy levels, temperature, and electronic density.

Plasma technologies work by energizing gas streams through electrical discharge (Fig. 3). This process results in the generation of various components, including positively charged ions, negatively charged electrons, neutrals, reactive and excited species, an electromagnetic field, and photons. In conditions that deviate from normal atmospheric pressure and temperature, these phenomena facilitate the efficient conversion of biomass into H<sub>2</sub> through oxidation.<sup>76,77</sup> Conversion methods utilizing plasma technology hold promise for the production of valuable chemicals in addition to H<sub>2</sub>, and their generation of harmful pollutants is virtually negligible.<sup>78,79</sup> Furthermore, by integrating with complementary processes, these methods can yield a H<sub>2</sub> product of exceptionally high purity.<sup>80</sup>

Kuo and colleagues<sup>75</sup> conducted a comprehensive analysis by a DC plasma torch reactor to evaluate the suitability of various biomass feedstocks for H<sub>2</sub> production. Their investigation encompassed a diverse range of sources, including pine wood chips, grape marc, forest residues, rice straw, and macroalgae. The chief aim of their research was to discern how the choice of biomass influenced not only H<sub>2</sub> production but also the formation of harmful compounds and the overall gasification yield achieved through plasma technology. Notably, the outcomes revealed a consistent H<sub>2</sub> concentration of 68 mol% in the syngas generated from all the studied biomass sources. Non-woody biomass sources showed a higher presence of sulfur compounds compared to woody sources, which can be explained by the inherent traits of non-woody materials. Among the tested options, pine wood emerged as the most favorable choice due to its exceptional efficiency in plasma gasification and the minimal presence of impurities in the resulting syngas, underlining its potential for sustainable H<sub>2</sub> production.

Wu and colleagues<sup>81</sup> conducted a comprehensive investigation into the presentation of methanol decomposition through a unique liquid-phase discharge setup, designed for enhanced visualization. The use of a high-speed camera in their study gave a detailed understanding of methanol decomposition and liquid-phase discharge processes. By changing the electrode spacing, the researchers were able to create two different plasma discharge modes: discharge (GD) and gliding arc



Table 2 A comparison between pyrolysis, gasification, and reforming in the production of green hydrogen

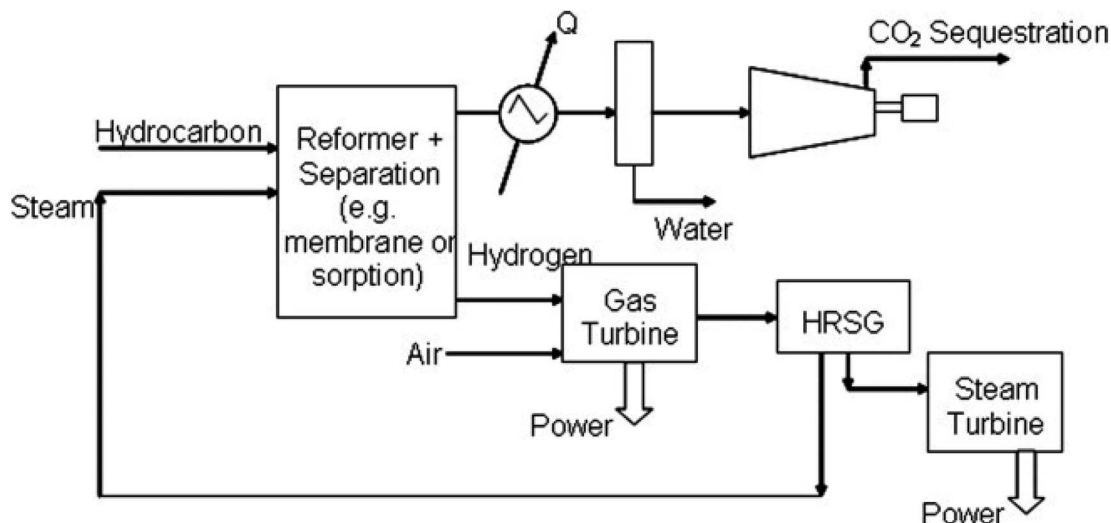
Type	Drawbacks	Benefits	Ref.
Pyrolysis	High required energy	High flexibility Fast and efficient feedstock decomposition	62–64
Gasification	Possibility of tar formation Need for high resistant equipment High required energy	H <sub>2</sub> -rich fuel production High productivity Ability to convert a variety of feedstocks	65–67
Reforming	Deactivation of electrodes Considerable reduction in electrode lifetime Need for catalyst regeneration High energy requirement	High potential to produce value-added products along with H <sub>2</sub> High-speed responding quality Cheap construction costs High capacity to reform varying materials Compactness	68–70

discharge (GAD) glow. GD's current and voltage curves closely resemble the sinusoidal waveform of AC power supplies, with a discharge power range of 130.4 to 460.2. In contrast, GAD exhibited a unique feature of bipolar pulses, characterized by high transient peak currents (ranging from 420.6 to 690.9 mA), resulting in a lower discharge power of 30.7–110.3 W. Initial analyses revealed that GAD's energy consumption was notably lower than that of GD, primarily because of disparities in their discharge characteristics. By optimizing the process, we achieved an energy consumption rate of 1.63 kW h per cubic meter of H<sub>2</sub> for hydrogen production. The result of this approach was a gaseous product with a maximum hydrogen proportion of 63.21%, and carbon monoxide as the primary byproduct at 26.38%. These findings shed light on an efficient and sustainable method for hydrogen production.

Tabu and their team<sup>82</sup> accomplished the development of low-temperature, atmospheric pressure plasma reactors utilizing the principles of gliding arc (glidarc) discharges and transferred arc (transarc). These reactors were meticulously designed, constructed, and meticulously characterized to facilitate the conversion of low-density polyethylene (LDPE), serving as a representative model for plastic waste, into H<sub>2</sub>. Their experimental findings revealed a clear relationship between voltage

levels and H<sub>2</sub> production rates and efficiency in both reactors. As voltage levels increased, H<sub>2</sub> production exhibited a steady rise. The transarc reactor achieved a maximum H<sub>2</sub> manufacture of 0.33 mmol g<sup>-1</sup> LDPE, while the glidarc reactor surpassed this with a peak hydrogen production of 0.42 mmol g<sup>-1</sup> LDPE. The transarc reactor showed increased hydrogen production with a narrower electrode-feedstock spacing. However, the glidarc reactor exhibited greater hydrogen generation when flow rates were moderate. Remarkably, despite their significantly different operational modes, both reactors delivered comparable H<sub>2</sub> production results. These findings represent a substantial step forward in the utilization of plastic waste for H<sub>2</sub> generation, offering valuable insights into the effectiveness of the transarc and glidarc technologies.

Conventional approaches to H<sub>2</sub> production encompass processes like water electrolysis, biomass gasification, coal gasification, and steam methane reforming. However, many of these methods, particularly those relying on fossil fuels, are associated with substantial carbon emissions, which run counter to the aim of achieving carbon neutrality. Future H<sub>2</sub> production should prioritize renewable resources and minimizing carbon emissions.<sup>83–85</sup>

Fig. 2 Representation of the SMR process.<sup>71</sup>

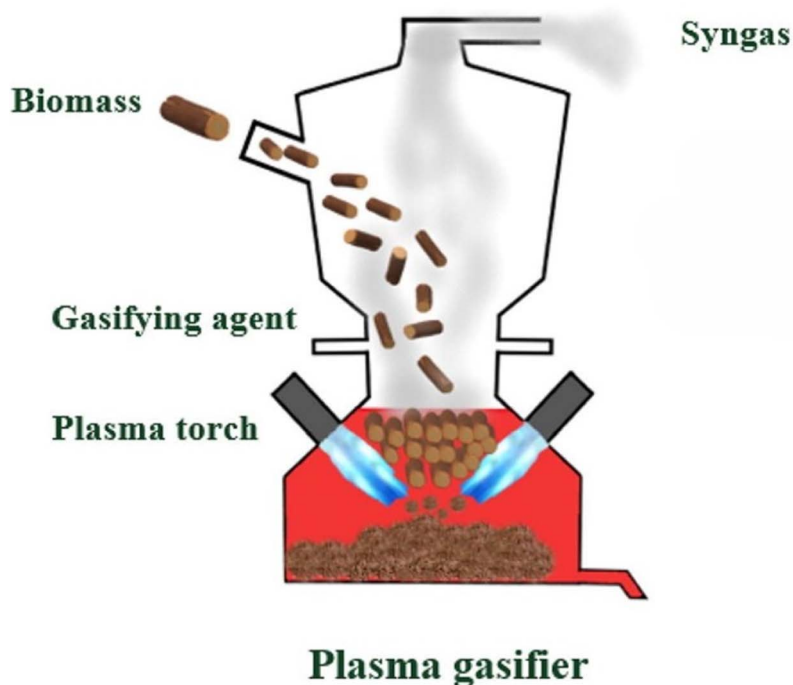


Fig. 3 Representation of the production of green H<sub>2</sub> with plasma route.<sup>75</sup>

### 2.3. Renewable energy-powered hydrogen generation systems

The efficient production of H<sub>2</sub> through renewable energy sources necessitates a thorough examination of the optimal configurations, which are contingent on factors for example geographical location, the obtainability of energy storage solutions, the choice between on-grid or off-grid systems, and the specific water electrolysis techniques employed.

Water electrolysis, despite being naturally endothermic, needs a higher voltage than the theoretical electrolysis voltage because of ohmic and overpotential loss.

In a study conducted by Gandia *et al.*<sup>87</sup> they conducted simulations to explore the production of H<sub>2</sub> through wind energy. Their findings revealed significant temperature fluctuations during transient operation, with notable temperature spikes observed under high-power generation conditions and, conversely, temperature decreases during low-power generation scenarios. Notably, the study identified a safety concern related to gas crossover, specifically the presence of O<sub>2</sub> in the H<sub>2</sub> stream and H<sub>2</sub> in the O<sub>2</sub> stream. The crossover gases reached high concentrations, especially when the gas volume decreased due to low power generation. This was mainly because the current determined the total of hydrogen gas manufactured. This underscores the importance of addressing safety considerations in H<sub>2</sub> production processes. Hence, the variability in the power supply altered the condition of the electrolyzer, impacting the purity of the gas produced.<sup>88</sup> Furthermore, The research by Ursúa *et al.* (Fig. 4),<sup>86</sup> they found that during the operation of an alkaline water electrolyzer without additional devices, a requirement was established to maintain a minimum power load of 40%. The objective is to maximize the employment of

renewable energy resources by evaluating if it's feasible to operate alkaline water electrolyzers below the minimum power load.<sup>86</sup> They aimed to improve the utilization of renewable energy sources. The outcomes of their study revealed that the system could sustain operation for up to 20 minutes under these conditions. Moreover, by implementing these adjustments, they were able to reduce the frequency of operational halts in a water electrolyzer powered by photovoltaic energy by half. Consequently, this approach led to an enhancement in energy efficiency by an additional 6.3%.

In their extensive research, Stansberry *et al.*<sup>89</sup> embarked on a series of experiments employing a 60 kW proton exchange membrane (PEM) water electrolyzer driven by a combination of wind power and photovoltaic sources. Within the complex system, the most significant energy loss, marked by the inadvertent release of hydrogen gas, was observed in the pressure swing adsorption dehumidification unit, closely followed by energy losses within auxiliary equipment and the power consumption associated with alternating/direct current (AC/DC) conversion units. The overall efficiency of water electrolysis was greatly affected by the accumulation of these losses, especially at lower electric power levels, resulting in a rated current drop below 50%. These fluctuations in power delivery resulted in similar adverse scenarios for the electrolyzers. As such, it becomes paramount to improve a comprehensive sympathetic of the mechanisms underlying the varying capabilities to support such fluctuating operations. This understanding can be attained by shedding light on the factors that dictate these abilities, which encompass factors like cell structures and the integration of auxiliary equipment. These insights are essential for improving the competence of water electrolysis in renewable energy systems.



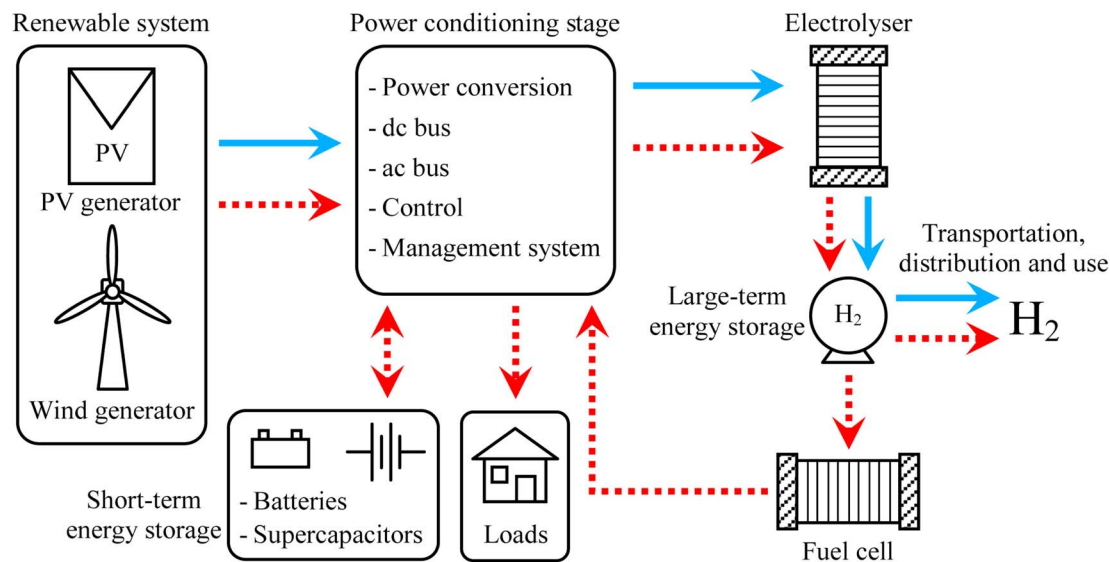
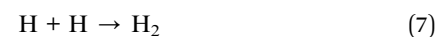
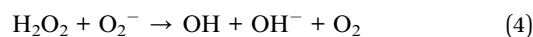
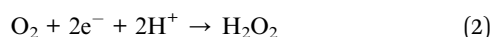
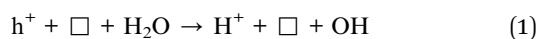


Fig. 4 Configurations for the integration of electrolyzers with renewable energies in stand-alone systems.<sup>86</sup>

Photovoltaic and wind energy production operate in diverse time cycles and exhibit varying power output fluctuations. These traits give rise to several challenges in the operation of electrolyzers. Notably, fluctuating power can lead to electrode degradation owing to abrupt shifts in electrode potential. A significant factor in this degradation is the reverse current generated during operational halts, resulting in a substantial deterioration of electrode performance.<sup>76</sup>

#### 2.4. Water splitting by photocatalysis

Harnessing the process of photocatalytic hydrogen production over water splitting shows promise as an environmentally friendly method for generating green H<sub>2</sub>, thanks to its cost-effectiveness and minimal energy requirements. The direct process of splitting water into O<sub>2</sub> and H<sub>2</sub> is thermodynamically challenging under standard ambient conditions, pressure off and temperature. The reaction is mainly caused by the high heat release, with a  $\Delta G$  of 237.1 kJ mol<sup>-1</sup> for water. It's worth mentioning that this reaction is not completely non-spontaneous and can be aided by catalysis.<sup>90</sup> Water splitting plays a pivotal role in producing clean and renewable H<sub>2</sub> for various applications, including H<sub>2</sub> fuel cells and energy storage, with minimal environmental impact since it does not produce harmful greenhouse gas emissions. The equations employed to represent the process of photocatalytic H<sub>2</sub> production are as provided below.<sup>91</sup>



The foundation of photocatalytic H<sub>2</sub> production lies in the semiconductor photocatalyst, which utilizes solar energy to split water. When light of a specific wavelength (a photons with a particular energy) strikes the photocatalyst, it energizes electrons from the valence band to the conduction band (CB). This event results in the creation of electron-hole (e<sup>-</sup>-h<sup>+</sup>) pairs, which play a pivotal role in driving the redox reactions occurring on the surface of the photocatalyst. Basic water splitting illustration is found in (Fig. 5).

Yan and his team,<sup>92</sup> achieved a remarkable milestone by developing a novel Ni<sub>2</sub>P/NiS@polymeric carbon-oxygen semiconductor (PCOS). Their work resulted in a groundbreaking achievement, with a notable production rate of 70.2  $\mu\text{mol h}^{-1}$  of O<sub>2</sub> and 150.7  $\mu\text{mol h}^{-1}$  of H<sub>2</sub> produced for every 100 mg of photocatalyst. Interestingly, the reaction solution also exhibited the presence of H<sub>2</sub> peroxide, initially at a rate of approximately 100  $\mu\text{mol h}^{-1}$  over the first 2 hours. This hydrogen peroxide had a detrimental impact on the photocatalyst's performance. However, the introduction of MnO<sub>2</sub> effectively mitigated this negative effect, resulting in excellent and stable rates of photocatalytic H<sub>2</sub> and O<sub>2</sub> production.

Ruan and colleagues (Fig. 6)<sup>93</sup> introduced a groundbreaking method that marks the inaugural attempt to leverage a straightforward ethylenediaminetetraacetate (EDTA) etching process. Their goal was to enhance the number of active surface sites on photocatalysts and reduce particle size, all while preserving high crystallinity. Among the tested materials, STO-2 demonstrated remarkable performance, achieving the highest activity levels. Specifically, it facilitated H<sub>2</sub> production at an impressive rate of up to 310  $\mu\text{mol g}^{-1} \text{h}^{-1}$  and O<sub>2</sub> evolution at 155  $\mu\text{mol g}^{-1} \text{h}^{-1}$ . What makes their work even more intriguing



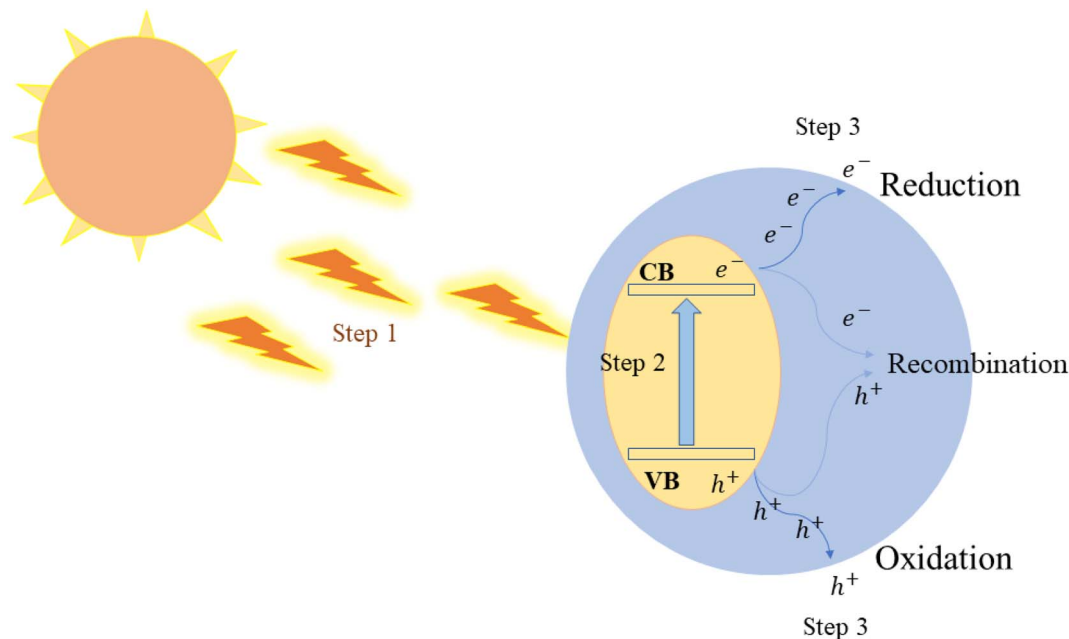


Fig. 5 Illustration of the photocatalyst water splitting process, (1) the absorption of light radiation from a light source, (2) the separation of electron–hole pairs, and (3) redox reaction.

is that the EDTA etching technique holds substantial promise for broader applications. Since EDTA can interact with a wide array of metals, this uncomplicated method has the potential to be further refined for the modification of various photocatalysts, enhancing their performance in a myriad of applications.

Saleh and the research team<sup>94</sup> delved into an exploration of various TiO<sub>2</sub> nanocomposites enriched with two co-catalysts: Cu or Pt nanocrystals in the 3–4 nm range. These nanocomposites were synthesized through different methods, including photo-

deposition, hydrothermal, and incipient wet impregnation. The results yielded a noteworthy discovery: the optimal H<sub>2</sub> generation occurred with a mass filling of 0.3 wt% for both co-catalysts. What's particularly remarkable is that, even in the absence of a precious metal like Pt, the Cu/TiO<sub>2</sub> nanocomposites, produced through the photo-deposition method, demonstrated a preliminary degree of 24 mmol h<sup>-1</sup> g<sup>-1</sup>. This rate was 3.5 times greater than those synthesized using the hydrothermal method and 1.4 times greater than those produced with the impregnation method. Conversely, for Pt co-

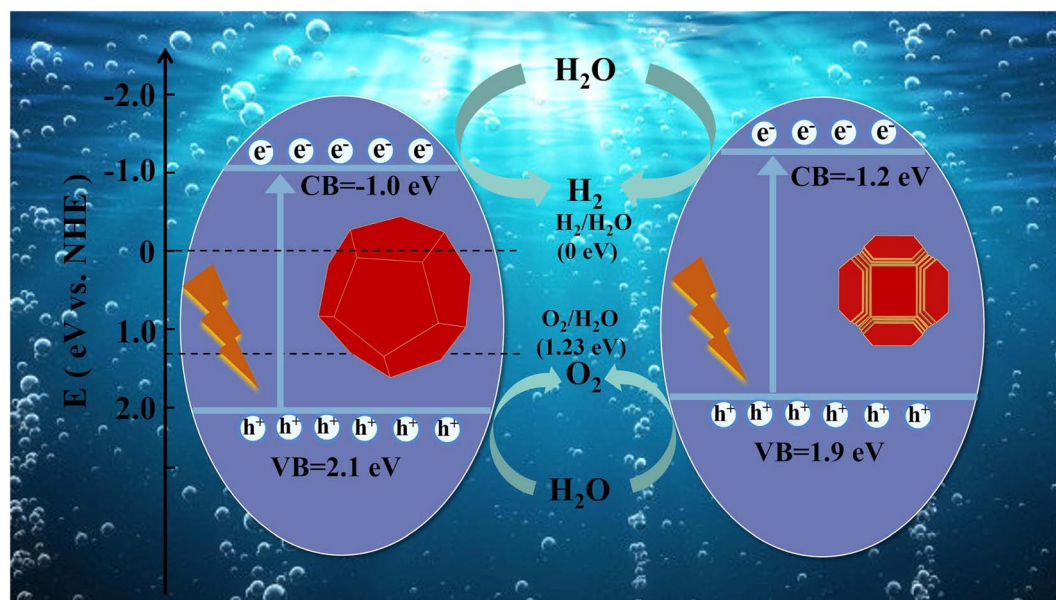


Fig. 6 Schematic diagram of photocatalytic water splitting of samples.<sup>93</sup>



catalysts, the highest rate was observed in the impregnation-synthesized composites, clocking in at  $58 \text{ mmol h}^{-1} \text{ g}^{-1}$ , surpassing the rates from the photo-deposition and hydrothermal synthesis methods by 1.6 and 1.1 times, respectively.

From (Table 3). The current analysis underscores that non-green methods of hydrogen production, including SMR and coal gasification, demonstrate superior efficiency and cost-effectiveness when compared to their green counterparts, such as electrolysis powered by renewable energy. Despite their environmental drawbacks, these conventional methods offer a more mature and economically viable pathway for large-scale hydrogen production in the immediate term. However, the urgent need to mitigate climate change and reduce greenhouse gas emissions necessitates a dual focus in future research endeavors.

It is imperative to enhance the cost-competitiveness and efficiency of green hydrogen production technologies. Significant advancements are required in areas such as electrolyzer technology, renewable energy integration, and novel catalyst development to bridge the gap between green and non-green hydrogen production. Furthermore, comprehensive cost-benefit analyses and life cycle assessments should be prioritized to ensure that the environmental benefits of green hydrogen are realized without compromising economic feasibility. Therefore, the next frontier in hydrogen research should aim to lower the production costs of green hydrogen while simultaneously improving its efficiency. This dual approach will not only facilitate a more sustainable hydrogen economy but also align with global environmental and economic goals. Only through such concerted efforts can we transition to a truly sustainable and scalable hydrogen infrastructure.

### 3. Storage

In the pursuit of efficient hydrogen storage solutions, researchers focus on several key material characteristics to ensure practical viability. High hydrogen storage capacity, both gravimetric and volumetric, remains paramount. Materials like metal hydrides and chemical hydrides, such as magnesium hydride ( $\text{MgH}_2$ ) and ammonia borane ( $\text{NH}_3\text{BH}_3$ ), respectively, offer substantial storage capacities. However, challenges such as the high temperatures required for hydrogen release in metal hydrides and the often-irreversible nature of chemical hydrides under practical conditions necessitate innovative approaches. Physisorption materials, like metal-organic frameworks (MOFs)

and carbon nanotubes, provide high surface areas and potential for low-temperature storage, though they typically require cryogenic conditions to achieve meaningful storage densities. Thus, achieving a balance between high capacity and operational practicality is essential.

Moreover, the kinetics of hydrogen absorption and desorption is a critical focus area, with researchers aiming to enhance these rates to facilitate rapid and efficient hydrogen storage cycles. This involves exploring nanostructured materials, which can offer increased surface areas and improved kinetics, and composite materials, which can tailor properties through synergistic interactions. Stability, both thermal and chemical, is also crucial to ensure durability over many cycles and to maintain performance without degradation. Safety and cost-effectiveness further underpin the practical deployment of these materials, necessitating that they be non-toxic, non-explosive, and economically viable for large-scale use. As such, the development of hydrogen storage materials is a multifaceted challenge, requiring a comprehensive approach to optimize capacity, kinetics, stability, and safety while maintaining economic feasibility.

The effectiveness of materials in storing  $\text{H}_2$  is closely tied to their physical and chemical characteristics, with a particular emphasis on their thermodynamic and kinetic properties.<sup>95</sup> Up to now, the predominant technological challenge in establishing a sustainable  $\text{H}_2$  economy has been the creation of effective  $\text{H}_2$  storage systems. When evaluating methods and materials for  $\text{H}_2$  storage, it's essential to consider various factors, including the design of high-pressure tanks, the densities of  $\text{H}_2$  in terms of weight and volume, refueling speed, energy efficiency, cost, durability, adherence to standards, technical readiness, and comprehensive assessments of both life cycle and efficiency.<sup>96</sup> To make  $\text{H}_2$  suitable for transportation, it's essential to enhance its energy density. Several methods have been suggested to achieve this, including liquefaction, compression, the formation of metal hydrides, and the utilization of liquid organic transporters such as conversion into energy carriers like methanol and ammonia.<sup>97,98</sup>

#### 3.1. Compressed hydrogen

Compression technology provides a direct approach to  $\text{H}_2$  storage. Nevertheless, this approach is noticeably ineffective in terms of volume and weight, due to the low density of compressed  $\text{H}_2$  – around 42.2 kg per cubic meter at 69.0 MPa. Extremely high pressures, reaching up to 70.0 MPa, are required

**Table 3** Energy efficiency, cost and characters of hydrogen production by different methods

Production method	Energy efficiency%	Production cost, € per kg $\text{H}_2$	Characters
SMR	70–85	0.56–1.12	High efficiency, low cost, mature technology, large emissions
Partial oxidation of methane	60–78	0.78–1.68	
Coal gasification	50–70	0.56–1.12	
Electrolysis of water (fossil energy)	62–82	1.79–3.36	High power consumption, high cost, high $\text{H}_2$ purity Zero emissions, high cost, low conversion rate
Wind electrolysis of water	—	—	
Solar electrolysis of water	—	—	



to achieve higher volumetric energy density in H<sub>2</sub> fuel cell electric vehicles, necessitating the use of tanks capable of withstanding such pressures. Currently, these high-pressure tanks are crucial for achieving a driving range similar to traditional fuel-powered vehicles.<sup>99</sup> Storing hydrogen in high-pressure tanks (up to 700 bar) is a mature technology. Innovations are focused on: (1) developing lightweight composite materials for tanks to improve gravimetric efficiency and safety, and (2) implementing advanced safety systems to monitor and control pressure and temperature, reducing risks of leakage and explosion.

### 3.2. Liquid hydrogen

Liquid H<sub>2</sub> presents itself as a suggesting option for efficient H<sub>2</sub> storage, mainly because of its exceptional purity and high density, which measures at approximately 70.8 kg of H<sub>2</sub> per cubic meter. The density of this is almost 800 times higher than that of uncompressed H<sub>2</sub> at standard temperature and pressure (0.08988 kg m<sup>-3</sup>). However, a significant drawback of H<sub>2</sub> liquefaction is the need for extremely low temperatures (around -253 °C), resulting in substantial energy consumption. Liquid H<sub>2</sub> becomes less feasible for long-term storage or transportation due to the cooling requirement. Another concern relates to the conversion of orthohydrogen to para-hydrogen, which generates heat through an exothermic isomerization process. The transformation of liquid H<sub>2</sub> into gaseous H<sub>2</sub>, known as the boil-off phenomenon, happens due to heat during storage and transportation.<sup>100</sup> Storing hydrogen as a liquid at -253 °C offers high energy density. Pathways for improvement include: (1) advancing cryogenic insulation materials and techniques to minimize boil-off losses, and (2) enhancing the efficiency of hydrogen liquefaction processes to reduce energy consumption.

### 3.3. Methanol

Storing H<sub>2</sub> and converting carbon dioxide through hydrogenation are both advantages of methanol. The 'power-to-product' concept often connects methanol with the use of renewable electricity to produce chemical fuels. Methanol can be employed to generate H<sub>2</sub> through processes such as steam reforming, thermolysis, and partial oxidation (POX).<sup>101,102</sup> However, the utilization of methanol as a means of H<sub>2</sub> storage poses environmental concerns at the point of use since it results in the release of CO<sub>2</sub> either directly or during its degradation. Additionally, the process of separating and capturing CO<sub>2</sub> comes with significant operational expenses and energy consumption. For instance, the conventional method of CO<sub>2</sub> separation and capture, involving the use of amine solutions, demands approximately 1.1 kW h per kilogram of CO<sub>2</sub>.<sup>103</sup>

### 3.4. Formic acid

The hydrogenation of CO<sub>2</sub> to form formic acid is an atom-efficient process that avoids water waste, making it a sustainable option for H<sub>2</sub> storage.<sup>104</sup> Additionally, formic acid exhibits promising characteristics as a H<sub>2</sub> carrier. It can store approximately 4.3% of H<sub>2</sub> by mass, and its high density, measured at 1.22 kg m<sup>-3</sup>, results in a significant volumetric density of 53 g

L<sup>-1</sup>.<sup>105</sup> When compared to alternative H<sub>2</sub> storage materials, the decomposition pathway of formic acid has garnered significant interest due to its low reaction enthalpy and the fact that it can be readily generated at temperatures as low as room temperature, up to 100 °C.<sup>106</sup> These features make formic acid a compelling candidate for H<sub>2</sub> storage solutions, especially when considering both its efficiency and practical storage capacities. As the pursuit of efficient and sustainable H<sub>2</sub> storage methods continues, formic acid stands out as a viable option with the hypothetical to diversion a fundamental part of the H<sub>2</sub> economy of the future.

### 3.5. Ammonia

In essence, effective H<sub>2</sub> carriers should possess a high H<sub>2</sub> content, offer ease of storage and transport, and readily decompose into H<sub>2</sub> when required.<sup>107</sup> NH<sub>3</sub> has garnered significant attention as a H<sub>2</sub> carrier due to its notable attributes, including a high H<sub>2</sub> content of 17.6 wt%, absence of carbon, and its ability to transition into a liquid state under mild conditions.<sup>108,109</sup>

Furthermore, NH<sub>3</sub> can be effectively broken down into a blend of N<sub>2</sub> and H<sub>2</sub> gases, resulting in the generation of larger quantities of high-purity H<sub>2</sub> while leaving no carbon footprint. This distinguishes it from hydrocarbon-based organic carriers like methane and methanol, which inevitably produce carbon dioxide. NH<sub>3</sub> also offers the advantage of being easier to maintain in a liquid state due to its lower boiling point compared with H<sub>2</sub> or methane. At room temperature, NH<sub>3</sub> can be liquefied with a moderate pressure of 1.0 MPa.<sup>110,111</sup>

Economic assessments have demonstrated that NH<sub>3</sub> holds greater promise in comparison to conventional fuels as methanol, liquefied petroleum gas (LPG), natural gas, gasoline, and hydrogen, primarily due to its absence of CO<sub>2</sub> emissions.<sup>112</sup> Furthermore, when compared to liquid H<sub>2</sub> (8.49 MJ L<sup>-1</sup>) and compressed H<sub>2</sub> (5.0 MJ L<sup>-1</sup> at 70.0 MPa and 25 °C), liquid NH<sub>3</sub> boasts a greater volumetric energy density, measuring at 10.5 MJ L<sup>-1</sup>.<sup>113</sup> NH<sub>3</sub> further distinguishes itself with a superior heat of combustion compared to liquid H<sub>2</sub> at 8.58 MJ L<sup>-1</sup> and nearly doubles the value of compressed H<sub>2</sub> at 5.0 MJ L<sup>-1</sup>. Additionally, NH<sub>3</sub> is less dense than air (0.769 versus 1.225 kg m<sup>-3</sup> at standard temperature and pressure). Under atmospheric conditions, gaseous NH<sub>3</sub> can disperse relatively quickly into the atmosphere, mitigating the potential explosion and fire hazards in case of accidental release. The fire risk is lower for NH<sub>3</sub> than H<sub>2</sub>, mainly because NH<sub>3</sub> has a higher auto-ignition temperature.<sup>114</sup>

### 3.6. Metal hydrides

A more feasible strategy is solid-state H<sub>2</sub> storage based on hydrides, which capitalizes on the reversible reactions that certain metals and alloys can undergo with H<sub>2</sub>.<sup>115,116</sup> Virtually all metallic elements have the capability to create binary compounds with H<sub>2</sub>, often referred to as elemental hydrides. Nevertheless, most of these compounds are not suitable for H<sub>2</sub> storage due to thermodynamics, H<sub>2</sub> storage capacity, or a combination of both factors.<sup>117</sup> The formation of hydrides presents a significant safety advantage in comparison to storage



methods involving pressurized gas and liquid H<sub>2</sub>, as it eliminates concerns about gas leakage. Ideally, hydrides should be capable of reversibly storing a substantial amount of H<sub>2</sub> (over 6.5 wt% H) under moderate conditions (at or below 80 °C) for on-board applications.<sup>118</sup> Metal hydrides, such as magnesium hydride (MgH<sub>2</sub>) and sodium alanate (NaAlH<sub>4</sub>), offer high volumetric hydrogen densities. Research should focus on: (1) incorporating alloying elements (*e.g.*, titanium or nickel) to reduce desorption temperatures and improve kinetics, and (2) developing nanoscale hydride particles to enhance surface area, reduce diffusion distances, and improve reaction rates.

**3.6.1. Factors affecting the choice of suitable metal hydride.** Various factors influence the selection of metal hydride materials for H<sub>2</sub> storage and compression. The intended application requires reversible hydride formation and decomposition within specific temperature and pressure ranges.<sup>119</sup> Additionally, the material must demonstrate a significant capacity to store and release H<sub>2</sub> under specific conditions. The pressure–composition–temperature (PCT) properties in H<sub>2</sub> gas systems affect these characteristics when interacting with hydride-forming materials. On the pressure-composition isotherm, the width of the plateau determines the reversibility of storage capacity. The direction of the process is contingent upon the correlation between current H<sub>2</sub> pressure and plateau pressure at the stated temperature. The plateau's inclination and the presence of hysteresis are important in H<sub>2</sub> compression applications. They cause a significant reduction in the compression ratio,<sup>120</sup> and affect the efficiency of the process within the specified temperature range.<sup>121</sup>

Selecting suitable metal hydride materials for high efficiency in reversible hydrogen storage and release involves considering several critical factors. First, the hydrogen storage capacity of the material is paramount; it should possess a high gravimetric (wt%) and volumetric capacity to store sufficient hydrogen. For instance, magnesium hydride (MgH<sub>2</sub>) offers a high hydrogen storage capacity of about 7.6 wt%. Secondly, the thermodynamics of the material, specifically the operating temperatures and pressures for hydrogen absorption (hydrogenation) and desorption (dehydrogenation), must be suitable for practical applications. A moderate enthalpy of formation is essential to balance storage capacity and ease of hydrogen release. Sodium alanate (NaAlH<sub>4</sub>), which operates at around 150 °C and 5 MPa, exemplifies favorable thermodynamics.

Kinetics is another crucial factor; the material should exhibit fast kinetics for both hydrogen absorption and desorption to minimize energy losses and reduce the time required for charging and discharging. For example, adding Ti-based catalysts to sodium alanate significantly improves its kinetics. Stability over multiple hydrogenation/dehydrogenation cycles is also vital, as the material must resist degradation and maintain its structural integrity and hydrogen storage capacity. LaNi<sub>5</sub>H<sub>6</sub> is noted for its good cycling stability and moderate operating conditions.

Safety and environmental impact are also key considerations. The material should be safe to handle, with minimal risk of toxicity or flammability, and should have a low environmental impact during production, use, and disposal.

Magnesium hydride, for instance, is relatively safe and environmentally benign compared to more reactive or toxic materials like lithium hydride. Cost and availability are important practical concerns; the material should be cost-effective and readily available for large-scale applications. MgH<sub>2</sub>, being abundant and inexpensive, is a popular choice for many applications.

Enhancements through additives and composites can significantly improve the performance of metal hydrides, enhancing their kinetics and thermodynamic properties. For example, mixing MgH<sub>2</sub> with transition metal catalysts like Ti or Ni can dramatically enhance its hydrogen absorption and desorption rates. Finally, the suitability of a material depends on the specific application, whether for stationary storage, mobile applications, or portable devices. LaNi<sub>5</sub>H<sub>6</sub>, with its moderate pressure and temperature requirements, is suitable for various applications, while MgH<sub>2</sub>, due to its higher operational temperatures, is more apt for stationary storage.

**3.6.2. Magnesium hydride.** There are many potential applications for MgH<sub>2</sub>, also referred to as magnesium hydride, as an energy carrier. It is cost-effective, widely available, and can store a lot of energy.<sup>122</sup> MgH<sub>2</sub> is a solid-state H<sub>2</sub> storage material. It has a high bulk density of 110 grams per liter and can hold an impressive weight capacity of 7.6% H<sub>2</sub> by weight. Additionally, it is known for its excellent safety and minimal environmental impact.<sup>123</sup>

Gao and colleagues<sup>124</sup> introduced a solid-solution MAX phase TiAlC catalyst directly into the MgH<sub>2</sub> system, without the need for etching treatment, to enhance H<sub>2</sub> storage performance. At 300 °C, the optimized MgH<sub>2</sub>-10 wt% TiAlC composite can absorb about 4.82 wt% of H<sub>2</sub> at 175 °C in 900 seconds and release around 6.00 wt% of H<sub>2</sub> in 378 seconds. Impressively, even after undergoing 50 isothermal H<sub>2</sub> absorption/desorption cycles, the composite exhibits exceptional cyclic stability and retains 99.6% of its capacity, which is 6.4 wt%. The abundant electron transfer at the external interfaces with MgH<sub>2</sub>/Mg is what gives the TiAlC catalyst its remarkable catalytic activity. Abundant electron transfer occurs at internal interfaces (Ti<sub>3</sub>AlC<sub>2</sub>/TiAlC) due to the presence of an impurity phase, Ti<sub>3</sub>AlC<sub>2</sub>, enhancing electron transfer and showing strong H<sub>2</sub> affinity. This study is the first to explore the impact of impurity phases, which are commonly found in MAX phases, on all catalyst activity. It provides a distinct method for designing composite catalysts that enhance the hydrogen storage capabilities of MgH<sub>2</sub>.

Li and his team<sup>125</sup> developed nanosheets of a medium-entropy alloy called CrCoNi. The addition of these nanosheets greatly boosted MgH<sub>2</sub>'s capacity for storing hydrogen at low temperatures. The dehydrogenation temperature of 9 wt% CrCoNi modified MgH<sub>2</sub> decreased by 130 °C from 325 °C to 195 °C, surprisingly. Additionally, the composite of MgH<sub>2</sub>-CrCoNi discharged 4.84 wt% of hydrogen in only 5 minutes at 300 °C and absorbed 3.19 wt% of H<sub>2</sub> in just 30 minutes at 100 °C (at 3.2 MPa). There was a decrease in activation energy by 45 kJ mol<sup>-1</sup> for dehydrogenation, and a decrease by 55 kJ mol<sup>-1</sup> for rehydrogenation. Through extensive cyclic kinetics analysis, it was discovered that the 9 wt% CrCoNi-doped MgH<sub>2</sub> showed



exceptional strength even subsequently 20 cycles, with a mere 0.36 wt% decrease in H<sub>2</sub> capacity. The stability of CrCoNi was confirmed by XRD patterns during the cyclic reaction process. Additionally, there was a uniform dispersion of CrCoNi nano-sheets on the surface of MgH<sub>2</sub>, resulting in numerous catalytic active sites and facile diffusion pathways with low energy barriers. Exceptional kinetic performance was achieved due to the synergistic catalysis that facilitated the rapid absorption and release of hydrogen atoms across the Mg/MgH<sub>2</sub> interface.

A novel technique was developed by Zhang and the research team<sup>126</sup> to boost the dehydrogenation and rehydrogenation capabilities of MgH<sub>2</sub>. The introduction of carbon-wrapped Ti and Co bimetallic oxide nanocages (Ti-CoO@C) made this possible. Through a precise hydrothermal method, the nanocages were synthesized and then mixed with MgH<sub>2</sub> using mechanical ball milling. The hydrogen desorption was notably influenced, as MgH<sub>2</sub> with 5 wt% Ti-CoO@C began desorbing hydrogen at 185.6 °C, a considerable 160.2 °C decrease compared to pure MgH<sub>2</sub>. Within a short span of 5 minutes, the composite released an astonishing 6.3 wt% H<sub>2</sub> at 275 °C. The MgH<sub>2</sub> + 5 wt% Ti-CoO@C composite exhibited a significant reduction in activation energy for H<sub>2</sub> desorption/absorption, dropping from 169.19 kJ mol<sup>-1</sup> and 83.61 kJ mol<sup>-1</sup> for MgH<sub>2</sub> to 137.76 kJ mol<sup>-1</sup> and 35.17 kJ mol<sup>-1</sup>, respectively. Furthermore, the composite displayed exceptional stability, with no significant decline in performance observed even after 20 cycles. The catalyst's even distribution and the *in situ* formation of titanium and MgO are responsible for the remarkable hydrogen storage performance. In addition, the promoting effect of Mg<sub>2</sub>Co/Mg<sub>2</sub>CoH<sub>5</sub> functioned as a H<sub>2</sub> pump, thereby contributing to the improved performance. Furthermore, carbon played a vital part in catalyst nanosizing and in reducing the strength of the Mg-H bond in MgH<sub>2</sub>. As a result, the 5 wt% Ti-CoO@C + MgH<sub>2</sub> composite exhibits outstanding hydrogen storage capabilities.

**3.6.3. Sodium alanate.** Sodium aluminum hydride, commonly known as NaAlH<sub>4</sub> and representing a class of materials known as alanates, is regarded as one of the greatest talented substances for solid-state H<sub>2</sub> storage. This is primarily attributed to its impressive H<sub>2</sub> storage capacity, which reaches as high as 7.5 weight percent. Beyond this notable feature, NaAlH<sub>4</sub> exhibits the remarkable ability to undergo reversible H<sub>2</sub> absorption and desorption processes under specific conditions.<sup>127,128</sup>

Ali and the research team<sup>129</sup> successfully developed CoTiO<sub>3</sub> through the solid-state method, and this novel material proved highly operative in ornamental the desorption behavior of NaAlH<sub>4</sub> for H<sub>2</sub> storage. The introduction of dissimilar weight percentages of CoTiO<sub>3</sub> (ranging from 5 wt% to 20 wt%) had a profound impact. NaAlH<sub>4</sub>'s initial desorption temperature significantly decreased due to the inclusion of CoTiO<sub>3</sub> catalysts. In the first desorption stage, the temperature decreased to about 130–160 °C, and in the second stage, it decreased to around 182–198 °C. These temperatures are much lower compared to untreated milled NaAlH<sub>4</sub>. The composite samples showed significantly faster desorption kinetics at 150 °C. A range of 3.0–3.7 was observed during the release of the NaAlH<sub>4</sub>-

CoTiO<sub>3</sub> composite. The activation energies for the two stages of NaAlH<sub>4</sub> desorption were greatly decreased. They were lowered to 85.5 and 91.6 kJ mol<sup>-1</sup>, which is a reduction of 30.7 and 35.5 kJ mol<sup>-1</sup> compared to untreated milled NaAlH<sub>4</sub>, respectively. The formation of Al-Co and Al-Ti alloys during the desorption of NaAlH<sub>4</sub>-CoTiO<sub>3</sub> is responsible for the remarkable catalytic effect of CoTiO<sub>3</sub>. These discoveries create new possibilities for the advancement of efficient catalysts for NaAlH<sub>4</sub>, showing its potential for H<sub>2</sub> storage purposes.

In a theoretical simulation by Mekky,<sup>130</sup> the research explored the characteristics of pure Na<sub>12</sub>Al<sub>12</sub>H<sub>48</sub>, and their variations with an interstitial doping of C, H, and Ti atoms. These clusters are being considered as a talented system for H<sub>2</sub> storage. The study found that, when compared to the interstitial space-doped clusters, the pure Na<sub>12</sub>Al<sub>12</sub>H<sub>48</sub> clusters exhibited greater stability. The introduction of interstitial space-doped C, Ti, and H atoms into Na<sub>12</sub>Al<sub>12</sub>H<sub>48</sub> did not significantly alter the lattice structure, and, notably, these atoms acted more than catalysts rather than traditional "interstitial space doping" elements. Additionally, the study found that the Na<sub>12</sub>Al<sub>12</sub>H<sub>48</sub> cluster displayed greater stability, but less chemical reactivity compared to the interstitial-doped clusters. When interstitial space-doped C, H, and Ti atoms were added to Na<sub>12</sub>Al<sub>12</sub>H<sub>48</sub>, the lattice structure remained largely unchanged. This confirms that Ti, C, and H atoms play a catalytic role rather than simply being interstitially doped into space.

Urunkar and their team<sup>131</sup> conducted a numerical analysis of a hydride reactor occupied with sodium alanate, specifically examining the absorption process within multiple tubes. They developed a mathematical model for the hydride reactor based on various governing equations and validated it using ANSYS Fluent. In general, water or oil is used in the hydride reactor to transfer heat while absorbing H<sub>2</sub>. The study replaced traditional heat transfer fluid with nanofluid for its better heat exchange properties. The research yielded results across several parameters, including the choice of nanoparticle material, nanoparticle concentration, H<sub>2</sub> supply pressure, and the inlet temperature of the heat exchange fluid. The absorption rate of the CuO/HTF nanofluid showed significant improvement, specifically at a 5 vol% concentration, surpassing other concentrations and selected nanofluids. This improvement translated to a 14% reduction in H<sub>2</sub> absorption time under specific conditions. Moreover, the CuO/HTF nanofluid with a 5 vol% concentration exhibited superior thermodynamic performance in comparison to other nanofluids, resulting in a 10% increase in heat exchange rate for the hydride reactor. The study found that the CuO/HTF nanofluid with a 5 vol% concentration performed better than the other nanofluids in the hydride reactor. This highlights the benefits of using nanofluids in this application.

The evaluation of various storage methods for green hydrogen reveals a diverse array of options, each with distinct advantages and challenges. Compressed hydrogen and liquid hydrogen offer straightforward and mature technologies but are hindered by high energy requirements and safety concerns related to pressurization and cryogenic temperatures. Chemical manufacturing of hydrogen carriers such as ammonia, methanol, and formic acid presents a promising alternative,



providing a more stable and potentially safer means of storage and transportation. However, these methods require further optimization to improve the efficiency of hydrogen release and to reduce associated carbon emissions. On the other hand, metal hydrides, including sodium alanate and magnesium hydride, demonstrate significant potential due to their high hydrogen storage densities and relatively moderate operating conditions. Nevertheless, the commercialization of metal hydride storage is currently limited by issues related to material cost, kinetics, and cyclic stability.

It is clear that while several methods show promise, no single storage technology currently meets all the criteria for widespread adoption. Therefore, ongoing research is essential to address the technical and economic barriers associated with each storage method. Future studies should focus on enhancing the efficiency of hydrogen release, reducing material costs, and improving the safety and feasibility of large-scale deployment. By advancing these areas, the development of an optimal hydrogen storage solution can be accelerated, thereby facilitating the broader adoption of green hydrogen as a key component of the global energy transition.

## 4. Applications

The H<sub>2</sub> economy is currently in existence, but it lacks environmental sustainability. Annually, the industrial sector is responsible for 6.3 billion metric tons of global energy-related carbon emissions.<sup>132</sup> About 17% (1.1 billion metric tons) of carbon emissions come from the production of gray H<sub>2</sub> feedstocks in chemical synthesis and industrial processes.<sup>133</sup> It's essential to produce cheap and carbon free hydrogen.

### 4.1. Domestic uses

When considering the use of hydrogen for domestic energy, one significant challenge is its lower volumetric energy density compared to natural gas. Hydrogen's energy content per unit volume is considerably less than that of natural gas, necessitating a larger volume of hydrogen to achieve the same energy output. This disparity impacts the efficiency and practicality of using hydrogen in residential settings, as it would require more substantial storage infrastructure and potentially more frequent refilling or supply mechanisms to meet household energy demands. Additionally, the existing natural gas infrastructure is optimized for the higher energy density of natural gas, meaning adaptations or new infrastructure investments would be necessary to accommodate the higher volumes of hydrogen needed for equivalent energy provision. Addressing this issue is crucial for integrating hydrogen as a viable energy source in homes, ensuring that it can be supplied efficiently and economically.

Hydrogen has 2.4 times more energy per unit mass than methane. However, due to its low density, its lower heating value (LHV) per unit volume is three times lower than methane. This results in a reduction of the energy content in the gas blend as the hydrogen concentration increases. From a safety perspective, higher hydrogen concentrations raise the risk of

fire and explosion. Hydrogen has a much broader flammability range (5.3 times) and detonation limit range (7.1 times) compared to methane. Additionally, it has a significantly lower ignition energy (14.5 times lower), making it more easily ignitable and increasing the fire risk.

Utilizing current pipeline systems to blend hydrogen with natural gas (Table 4) offers the most affordable means of transporting significant quantities of hydrogen over long distances without requiring new infrastructure. Nonetheless, because hydrogen molecules are smaller and have unique physical characteristics, including lower density and viscosity, the mixture exhibits behavior distinct from that of pure natural gas.<sup>139,140</sup> This introduces potential safety hazards for pipelines designed specifically for natural gas. To keep the energy output consistent, the mixture with hydrogen may require higher flow rates, leading to increased operating pressures that could surpass the design limits of the compressors and pipelines originally meant for natural gas. Hence, it is essential to consider redesigning these systems to safely transport the hydrogen blend and to identify any risks and operational challenges associated with varying hydrogen concentrations. It is crucial to maintain a uniform mixture of the blended gas along the entire pipeline. Significant density differences between the gases can cause them to separate, leading to varied flow behaviors and leak issues. This separation can result in inconsistent energy distribution and operational challenges in the pipeline.<sup>134</sup>

M. Ozturk *et al.*,<sup>142</sup> designed and studied an integrated system to produce renewable hydrogen and blend it with natural gas from the Black Sea for widespread use in Turkey. They focused on a case study for the city of Zonguldak, aiming to use the natural gas reserves more efficiently and environmentally. The study primarily investigates blending natural gas with 20% hydrogen by volume. Renewable energy sources such as wind, solar, and wave were evaluated for their hydrogen production capacities, yielding 1432 kg, 174 210 kg, and 1257 kg, respectively. The study examined the impact of this hydrogen addition on gas consumption and the lifespan of natural gas reserves. With 20% hydrogen, annual gas consumption increased from 46.55 billion cubic meters (bm<sup>3</sup>) to 54.11 bm<sup>3</sup>, while natural gas consumption decreased from 46.55 bm<sup>3</sup> to 43.29 bm<sup>3</sup>, extending the reserve lifespan from 11.6 years to 12.5 years. Emissions of CO and CO<sub>2</sub> dropped significantly, from 0.05 g day<sup>-1</sup> and 32% to 0.02 g day<sup>-1</sup> and 28%, respectively, as the hydrogen content increased from 5% to 20%. However, NO<sub>x</sub> emissions rose from 4.08 g day<sup>-1</sup> to 7.54 g day<sup>-1</sup> with the same hydrogen increase.

Table 4 Hydrogen blending system<sup>134–138</sup>

Project	Country	Network	Electrolyser capacity	Hydrogen blend %
HyP SA	Australia	Distribution	1.2 MW	5%
ATCO-CEIH	Australia	Distribution	0.15 MW	5–25%
HyDeploy	UK	Distribution	0.5 MW	20%
Jupiter 1000	France	Transmission	1.0 MW	6%



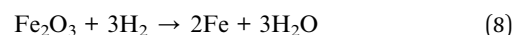
M. Ozturk *et al.* (Fig. 7),<sup>141</sup> conducted an experimental investigation to analyze the impact of adding hydrogen to natural gas on emissions and combustion performance. They burned natural gas and various natural gas-hydrogen blends (with 10%, 20%, and 30% hydrogen by volume) in identical gas stoves and measured emissions of CO, CO<sub>2</sub>, and NO<sub>x</sub>. The results showed that increasing the hydrogen content improved combustion efficiency from 39.32% to 44.4%. Higher hydrogen ratios reduced CO<sub>2</sub> and CO emissions, but NO<sub>x</sub> emissions varied. A life cycle analysis assessed the environmental impact of the different blending scenarios. With a blend containing 30% hydrogen, the global warming potential decreased from 6.233 to 6.123 kg<sub>CO<sub>2</sub></sub> equivalents per kg<sub>blend</sub>, and the acidification potential dropped from 0.0507 to 0.04928 kg<sub>SO<sub>2</sub></sub> equivalents per kg blend compared to pure natural gas. However, there were slight increases in human toxicity, abiotic depletion, and ozone depletion potentials per kg blend, rising from 5.30 to 5.52 kg 1,4-dichlorobenzene (DCB) equivalents, 0.0000107 to 0.00005921 kg Sb equivalents, and  $3.17 \times 10^{-8}$  to  $5.38 \times 10^{-8}$  kg CFC-11 equivalents, respectively.

#### 4.2. Steel manufacturing

The global steel industry currently uses approximately 5% of the world's energy and contributes over 6% of annual human-caused CO<sub>2</sub> emissions.<sup>143,144</sup> Approximately 15% of China's

total CO<sub>2</sub> emissions come from the steel industry.<sup>145</sup> In China, more than 90% of crude steel is manufactured using the blast furnace-converter process, which relies heavily on coal-based energy sources. Due to the significant demand for steel products and its economic viability, this method is expected to remain the prevailing approach in the coming decades.<sup>146</sup>

In the steel industry, hydrogen serves two main purposes: (1) reducing iron oxide content in the blast furnace (BF) production process and the gas-based direct reduction iron (DRI) process, (2) it functions as a fuel for various heating applications, such as assisting in sintering production, the pelletizing process, and heating ladle furnaces, among others.<sup>147,148</sup> Introducing hydrogen-enriched gases into the BF results in a reduction in the viscosity and density of the gas mixture. This reduction in density and viscosity leads to a lower pressure drop and faster heat exchange between the gas mixture and the materials being processed in the BF. As a result, this contributes to enhancing the efficiency of heat utilization in the BF.<sup>147</sup> Simultaneously, during the reduction in iron oxides by hydrogen eqn (8), the diffusion capacity of hydrogen is 3.74 times greater than that of carbon monoxide. The internal micro and macro pores of the iron ores enable H<sub>2</sub> to efficiently reach the reaction interface through diffusion.<sup>149</sup> Consequently, if the H<sub>2</sub>/CO ratio is higher, the reduction rate will be faster with the same volume fraction of reduction agents. Numerous scholars have substantiated this through studies on the dynamic aspects of iron oxide reduction.<sup>147,150–155</sup>



It was clear now that hydrogen metallurgy offers several advantages. Firstly, it produces H<sub>2</sub>O as a reduction product, reducing reliance on fossil fuels like coal and coke and decreasing CO<sub>2</sub> emissions. Additionally, H<sub>2</sub> serves as a superior reductant compared to CO, thanks to its higher calorific value, lower density, enhanced penetration, and faster reduction rate. The availability of abundant raw materials for H<sub>2</sub> production ensures a readily available supply. Moreover, H<sub>2</sub> metallurgy can stimulate the rapid growth of DRI processes by substituting natural gas with H<sub>2</sub>, which is valuable in localities with limited natural gas resources, such as China. In general, H<sub>2</sub> metallurgy plays a role in the sustainable development of iron and steel enterprises.

#### 4.3. Chemical manufacturing (methanol, methane, green ammonia, formic acid)

Conventional coal chemical production exhibits low energy efficiency and significant CO<sub>2</sub> emissions. Coal has a hydrogen-to-carbon (H/C) ratio of approximately 4 : 5, while the resulting chemical products like natural gas, liquid fuels, olefins, and methanol have H/C ratios of around 3 : 1, 2 : 1, 2 : 1, and 2 : 1, respectively.<sup>156,157</sup> The disparity in H<sub>2</sub> and carbon content between chemical and coal products results in an excess of carbon and substantial CO<sub>2</sub> emissions during coal conversion processes. Take the coal-to-methanol (CTM) conversion as an example, where the gas produced from coal gasification has an H/C ratio of around 0.7, while synthesized methanol has a ratio

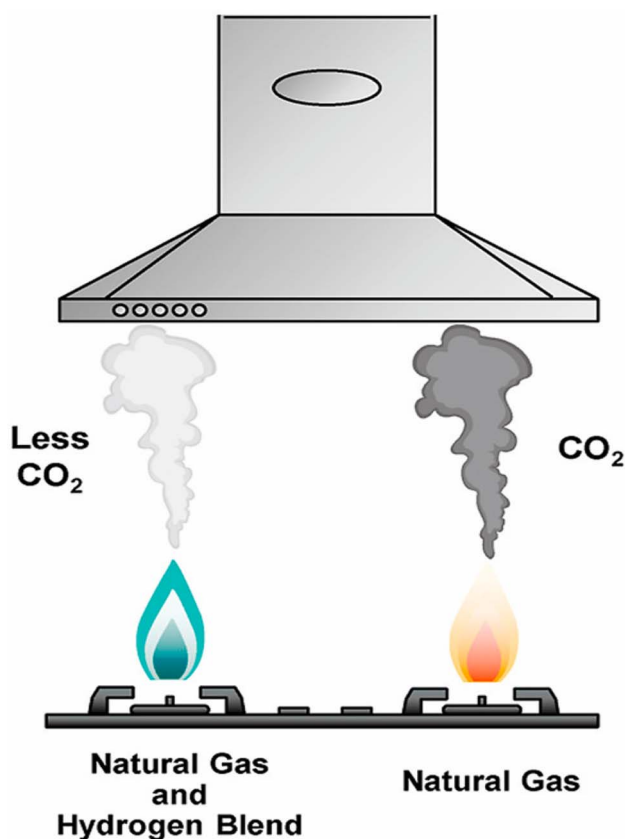


Fig. 7 Illustration of the benefit from blending green H<sub>2</sub> with natural gas.<sup>141</sup>



of about 2.0. The conversion of CO to H<sub>2</sub> necessitates the water-gas shift reaction. During this process, the majority of the carbon is converted into CO<sub>2</sub> and then emitted into the atmosphere. As a result, carbon resources are wasted and significant CO<sub>2</sub> emissions are generated.<sup>158,159</sup> Approximately 45% of energy is efficiently used in the CTM process, with CO<sub>2</sub> emissions ranging from 3.8 to 4.3 metric tons per metric ton of methanol.<sup>160,161</sup> As shown in (Fig. 8) green hydrogen is a great candidate for manufacturing various chemical compounds such as ammonia, methane, methanol, formic acid and so on without releasing carbon dioxide as in (Fig. 9).

**4.3.1. Methanol.** Methanol (Fig. 10a) is used as a crucial raw material in producing different chemicals, including methyl *tert*-butyl ether, acetic acid, dimethyl ether, formaldehyde, and various products like plastics, paints, construction materials, and automotive components.<sup>162</sup> It is known for its versatility as a solvent and low-emission synthetic fuel used in various applications, such as wastewater treatment, cooking, industrial boilers, transportation, and electricity generation. Additionally, it serves as a carrier for chemical energy in fuel cells and an alternative medium for transporting H<sub>2</sub>.<sup>162,163</sup> The traditional method involves fossil fuel-based synthesis gas, but it can also be produced by directly oxidizing natural gas or reducing atmospheric CO<sub>2</sub> with H<sub>2</sub>. Producing green methanol by combining H<sub>2</sub> and CO<sub>2</sub> offers a way to reduce greenhouse gas emissions. This methanol can serve as both a sustainable transportation fuel and a means to store electricity.<sup>164</sup>

Dongliang and colleagues<sup>165</sup> introduced an innovative approach for H<sub>2</sub> production coupled with CO<sub>2</sub> application in the coal-to-methanol (CTM) process. They termed this new approach the GH-CTM process, designed to enhance material integration, carbon efficiency, and methanol yield. Through comprehensive process modeling, parameter optimization, and simulations, the results demonstrated remarkable improvements compared to the conventional CTM process. The GH-CTM process exhibited a 10.52% higher energy efficiency, an 85.64% reduction in CO<sub>2</sub> emissions, and a remarkable 124.67% increase in methanol production. In addition, the proposed

process had significantly slowed production costs, 23.95% less than the traditional CTM process. Notably, the payback period for investment in the GH-CTM process was substantially shorter, at 2.8 years, compared to the CTM process's 7.2 years. Moreover, the GH-CTM process experienced a 47.37% increase in internal rate of return compared to the traditional CTM process. This new approach shows potential for introducing green H<sub>2</sub>, utilizing CO<sub>2</sub>, and transforming coal into valuable chemicals sustainably.

A preliminary assessment by Sollai and their team<sup>166</sup> looked into a power-to-fuel plant setup for generating 500 kg h<sup>-1</sup> of renewable methanol using green H<sub>2</sub> and captured CO<sub>2</sub>. They developed a comprehensive process model employing the Aspen Plus tool, which simulated all aspects of the plant and the system as a whole. Once the process was optimized, a comprehensive economic analysis was performed, considering operating and capital costs derived from real-world experience at a commercial scale, with a projected operational lifetime of 20 years. Through the analysis, it was determined that the LCoM is 960 € per t, which translates to around 175 € per MW h. While the study showed that, as of the present, the technology isn't yet economically competitive, with the LCoM exceedingly double the prevailing international methanol price of 450 € per t, it does indicate a potential shift towards competitiveness in the medium-term future, largely driven by evolving European policies. Additionally, the research revealed that LCoM is particularly influenced by factors such as electricity prices, electrolyzer capital costs, and the plant's capacity factor.

**4.3.2. Green ammonia.** Over the past ten years, global ammonia (Fig. 10b) production has experienced significant expansion, primarily driven by the top five nations, including Indonesia, the USA, India, Russia, and China, which collectively contribute to approximately 60% of the overall market. The exothermic reaction between nitrogen and hydrogen leads to ammonia synthesis, as shown in equation.<sup>167</sup>

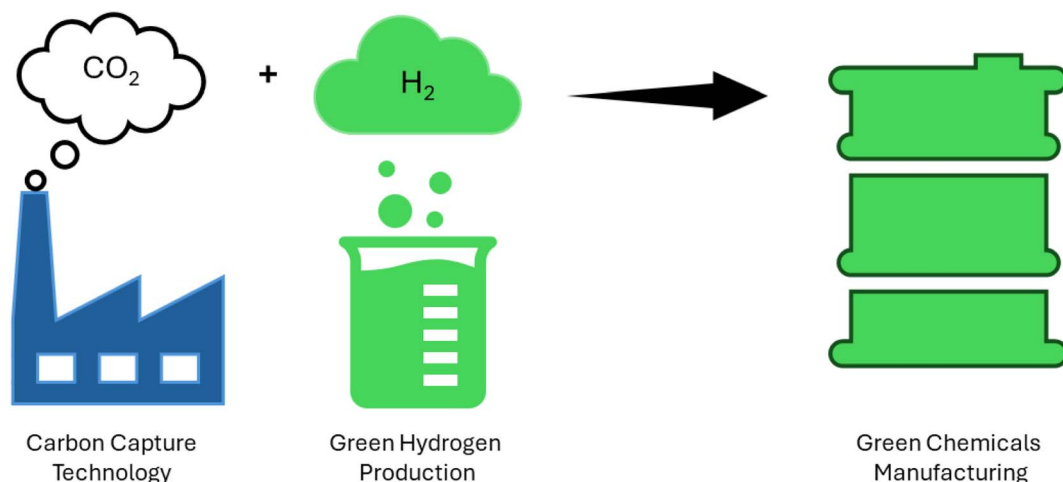
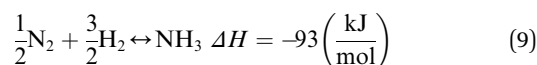


Fig. 8 Illustration of the manufacturing of different organic materials using carbon capture and green hydrogen production.



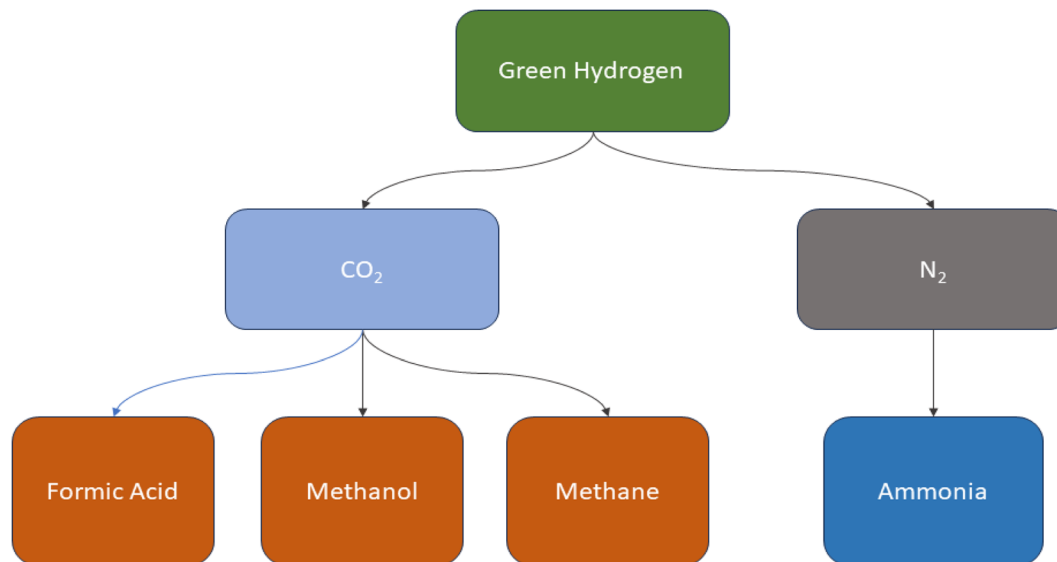


Fig. 9 Showing the different chemical products that can be generated by green H<sub>2</sub>.

As outlined by MacFarlane *et al.*,<sup>168</sup> various approaches for green ammonia production can be categorized: First-generation green ammonia involves capturing carbon emissions post-ammonia production and storing it, resulting in what is referred to as “blue ammonia”. Second-generation green ammonia focuses on producing ammonia from environmentally friendly feedstocks, namely N<sub>2</sub> and H<sub>2</sub>. This approach aims to transform the traditional Haber–Bosch process into a sustainable source. Third-generation green ammonia entails departing from the conservative Haber–Bosch process and adopting alternative methods that prioritize high stability, sustainability, and the use of renewable sources for ammonia production.

Currently, various methods exist for the indirect generation of environmentally friendly ammonia, such as microbial electrolysis,<sup>169</sup> photosynthesis,<sup>170</sup> dark fermentation,<sup>171</sup> and electrolysis.<sup>172</sup> Electrochemical techniques have garnered significant attention in numerous nations.<sup>173</sup>

An enhanced optimization-based simulation model was introduced by Zhao and their team<sup>174</sup> to simulate the long-term sustainability of green manufacturing. They investigated the effect of significant institutional incentives and the collaborative effects of O<sub>2</sub> on investments. According to the study, the estimated levelized cost of ammonia is about 820 USD per t, which is nearly twice the current market price. Several factors were identified as pivotal in green ammonia investments,

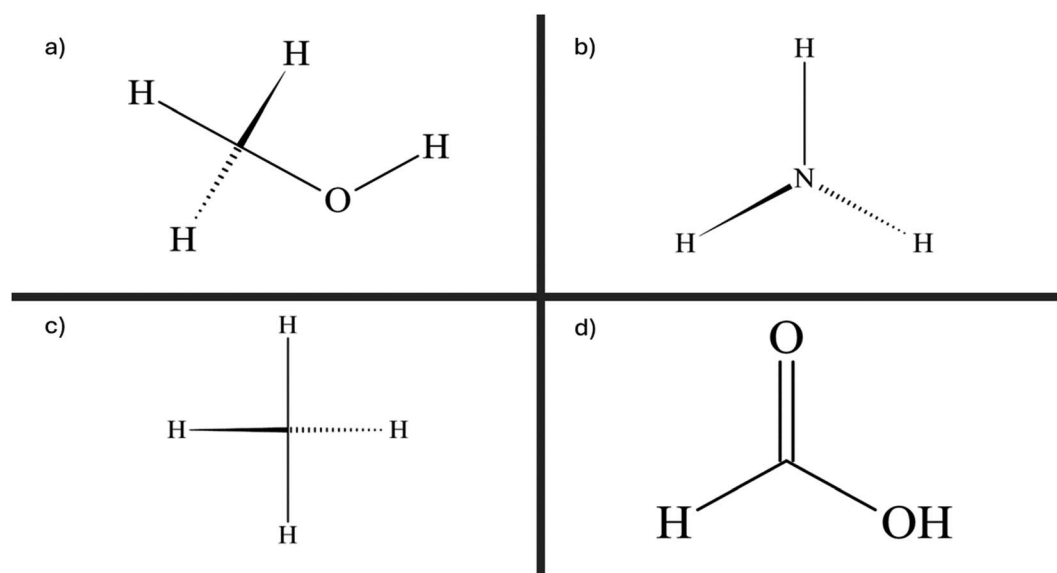


Fig. 10 Visual representation of the chemical structure of (a) methanol, (b) ammonia, (c) methane, and (d) formic acid.



including the operational rate, the electrical efficiency of electrolyzers, electricity costs, and ammonia pricing. China's energy transition was greatly influenced by carbon pricing and VAT exemptions. To bridge the gap, a subsidy of about 450 USD per t would be needed based on the current pricing, but this could be lowered by 100 USD per t through the implementation of O<sub>2</sub> synergy. Comparatively, green NH<sub>3</sub> production exhibited both environmental and economic advantages when contrasted with inter-regional power transmission. The study thus advocates a balanced approach, leveraging both options to address integrating O<sub>2</sub> manufacturing into H<sub>2</sub> production and renewable power curtailment processes. By mitigating renewable power curtailment, this research aims to encourage the increase of the H<sub>2</sub> economy in China.

Ishaq and colleagues<sup>175</sup> conducted a study to determine if offshore wind energy can be used to produce green ammonia and green H<sub>2</sub>. They used water and air as the main inputs. The green ammonia would then be transferred to onshore demand points using ships or pipelines. They performed a comprehensive year-long transient analysis to ensure the technology's reliability and adherence to quality standards before field deployment. Their approach involved integrating offshore wind energy with a water electrolysis unit and a seawater desalination system to generate renewable H<sub>2</sub> for subsequent green ammonia synthesis. In terms of costs, the economic analysis revealed that the offshore wind farm and electrolyzer made up the majority, with 45% and 29% allocations, respectively. In order to meet the constant demand for green ammonia at a rate of 554 kg h<sup>-1</sup>, they concluded that an 80 000 kg H<sub>2</sub> storage system was necessary, which could also provide ammonia to external customers. The study further illustrated the variations in ammonia production capacity over the course of the year, both with and without the H<sub>2</sub> storage system. Importantly, it demonstrated that integrating a H<sub>2</sub> storage system could ensure a steady supply of green ammonia throughout the year.

Bouaboula and the research team<sup>176</sup> developed a new Techno-Economic (TE) modeling method. Their goal was to optimize the operation and design of a pilot-scale Green Ammonia plant. The intermittent nature of renewable energy sources is taken into account in this novel TE model. In order to deal with this, we examined multiple site locations that had consistent meteorological data each year. Furthermore, the model includes a unique Energy Management Strategy (EMS) to ensure a continuous power supply for the Haber–Bosch (HB) reactor. The EMS ensures the smooth distribution of power from renewable sources to charge and discharge Energy Storage Systems (ESS). Two main Key Performance Indicators (KPIs) were used to evaluate the plant's performance: Levelized Cost of Ammonia (LCOA) and HB Load Factor (LF). The findings indicated that the implemented EMS effectively reduced the fluctuations in RE sources by optimally distributing power across different time slots. Consequently, the HB LF rose by 56% to 65%, based on the particular RE setup. The increase in LF resulted in lower plant costs due to higher production yield outweighing investment and operational expenses. The PV/Battery scenario, consisting of 6 MW of PV and 11 MW h of battery capacity, was identified as the most efficient plant

configuration, with a LCOA of \$774 per t NH<sub>3</sub>. By 2050, the estimated cost of NH<sub>3</sub> could decrease to \$250 per ton according to a forecast. Furthermore, it suggests that green ammonia is expected to be economically competitive with conventional fossil fuel approaches by 2030.

**4.3.3. Green methane.** Methane (Fig. 10c) (CH<sub>4</sub>), often referred to as synthetic natural gas (SNG), is a readily available fuel found in nature, being the primary component of natural gas. Despite its status as a significant greenhouse gas, methane finds utility in electricity generation and industrial chemical processes, where it's burned in steam generators and gas turbines. It also plays a substantial role in our daily lives, serving as fuel for ovens, water heaters, kilns, automobiles, and more.<sup>177</sup> When compared to other hydrocarbon fuels, CH<sub>4</sub> is known for its significantly lower CO<sub>2</sub> emissions, making it a more environmentally friendly option.<sup>178</sup>

Pignataro *et al.*<sup>179</sup> presented three management strategies (MSs) for controlling the H<sub>2</sub> storage tank and methanation unit in the power-to-gas system. The most influential operational variables were determined through a systematic comparison of these MSs, and their impact on system performance was evaluated. The first strategy, denoted as MSA, stood out as the most straightforward of the three. When the produced H<sub>2</sub> falls within the operational range, MSB closely resembled MSA in its behavior when operational constraints were breached. The control algorithm of MSC was similar to MSB, but the storage tank supplied different amounts of additional H<sub>2</sub> during “in-range” methanation operations. While the methanation unit was running, we considered a scenario where the setpoint for methanation matched the flow rate from the electrolysis system (ES). The findings indicated that MSA and MSB exhibited similarities in the methanation unit and CH<sub>4</sub> production utilization factor. Despite this, MSB demonstrated greater efficiency in handling methanation unit shutdowns, albeit with the drawback of needing a bigger storage system. On the other hand, MSC demonstrated the highest CH<sub>4</sub> production but had more shutdowns and used a smaller storage system. Nonetheless, the results consistently showed a low average state of charge (SOC) for the storage in all MSs, suggesting that the system components may not have been sized optimally. Further investigation is needed to explore how resizing different subsystems impacts system performance and cost. Ultimately, the selection of the management strategy varies on the goal and feasibility of utilizing excess H<sub>2</sub> in the power-to-methane system.

In a comprehensive study, Garcia-Luna *et al.*<sup>180</sup> focused on integrating waste biomass oxycombustion with a power-to-methane system. Their approach primarily relies on using photovoltaic solar energy to drive PEM electrolysis and produce H<sub>2</sub> and O<sub>2</sub>. The gases are utilized in a sub-critical steam power cycle for waste combustion. Depending on the operational strategy, an air separation process utilizing cryogenic distillation can generate an extra O<sub>2</sub>. Following purification and compression, the CO<sub>2</sub> stream is directed towards the methanation reactor. The researchers created a quasi-stationary model to simulate the entire plant and assess integration efficiency under different operational conditions. According to



their study, the entire plant integration shows high efficiency, with a CO<sub>2</sub> reduction associated efficiency penalty of approximately 6% points on average per year. The system reduces emissions by using waste biomass as the primary fuel source, resulting in a -610 kg<sub>CO<sub>2</sub></sub> per MW h reduction compared to biomass plants without CO<sub>2</sub> capture. Furthermore, a comprehensive annual techno-economic study shows an average levelized electricity cost of €56 per MW h and an average green CH<sub>4</sub> production cost of €12 per MW h. The results support the implementation of this system in both new and retrofitted biomass power plants because the CO<sub>2</sub> capture cost is around 65.66 € per ton of CO<sub>2</sub>.

**4.3.4. Formic acid.** Formic Acid (FA) (Fig. 10d) is a clear and intensely sharp-smelling liquid when maintained at standard room temperature and atmospheric pressure. It possesses the property of miscibility with water and a wide range of polar organic solvents, while showing partial miscibility with hydrocarbons. This versatility in solubility is attributable to its dual characteristics, featuring both acid and aldehyde functional groups, rendering it inherently reducing in nature.<sup>181</sup> FA, recognized as a pivotal platform chemical, holds significant importance in both the chemical and agricultural sectors. In particular, it serves as a fundamental chemical compound extensively employed across various industries, including but not limited to chemical, textile, leather, pharmaceutical, and rubber industries.<sup>182,183</sup> In the past decade, silage preservation and the use of formic acid as an additive in animal feed have outpaced its application in leather and tanning, making it the most significant global utilization of this compound.<sup>183</sup>

Gong and his team<sup>184</sup> developed an advanced integrated system that merges methanol selective oxidation reaction and the H<sub>2</sub> evolution reaction. By incorporating a power management system, this system operates on a UDC RF-Pulsed-TENG. At the cathode, green H<sub>2</sub> is produced in this setup, while simultaneously generating the high-value chemical product, FA, at the anode. Applying a constant voltage of 1.8 V to the electrochemical cell after power management resulted in 1.68 times increase in the green H<sub>2</sub> production rate. The entire system produces green H<sub>2</sub> at a rate of 14.69 μL min<sup>-1</sup> with 100% Faraday efficiency. Additionally, it allows for the simultaneous and quick generation of pure green H<sub>2</sub> and valuable FA using clean energy sources.

#### 4.4. Hydrogen fuel cells

Developed in 1839, fuel cells represent electrochemical devices with the remarkable ability to convert H<sub>2</sub> and O<sub>2</sub> directly into electricity, all while operating in an environmentally friendly manner, free from CO<sub>2</sub> emissions. These devices present a compelling alternative, holding the promise of steering us towards a future of decarbonized energy solutions.<sup>185</sup> Fuel cell technology consists of a trinity of key components: the cathode, the electrolyte, and the anode. Here, the anode plays a vital role, as H<sub>2</sub> engages in an oxidation reaction ( $\text{H}_2 \rightarrow 2\text{H}^+ + 2\text{e}^-$ ), setting free electrons in motion through an external circuit, while positively charged cations make their way towards the cathode by traversing the electrolyte. It's at the cathode that

a critical reduction reaction unfolds ( $4\text{H}^+ + \text{O}_2 + 4\text{e}^- \rightarrow 2\text{H}_2\text{O}$ ), involving both cations and electrons, ultimately converting O<sub>2</sub> into water. These orchestrated chemical reactions are the cornerstone of fuel cell power generation.<sup>186</sup> Cells that can serve as both fuel and electrolyzers cells within a single system are known as regenerative reversible or fuel cells. They derive this capability from their ability to reversibly split and recombine water ( $\text{H}_2\text{O} + \text{energy} \leftrightarrow \text{H}_2 + \frac{1}{2}\text{O}_2$ ).<sup>187</sup> Fuel cells offer a range of benefits, including adaptability, a modular structure, impressive energy density (ranging from 300 to 1200 Wh kg<sup>-1</sup>), strong power output, robust cycling performance, excellent thermal and mechanical stability, a prolonged lifespan (capable of enduring 20 000 or more discharge/charge cycles over 15 years), minimal vibration and noise, cost-effective maintenance, and straightforward installation and transportability.<sup>188,189</sup> Nonetheless, the main hurdles for implementing this technology on a large scale revolve around the substantial upfront expenses and the complexities associated with widespread deployment.<sup>190</sup> Different types such as molten carbonate fuels (MFCs), phosphoric acid fuel cells (PAFCs), alkaline fuel cells (AFCs), proton exchange membrane fuel cells (PEMFCs), and solid oxide fuel cells (SOFCs) are compared in Table 5.<sup>191</sup>

## 5. Economics

The notion of a “H<sub>2</sub> economy” was initially formulated by John Bockris during the 1970s. The idea is to produce H<sub>2</sub> by electrolyzing water and then distribute it through pipelines to different locations. These locations would utilize on-site fuel cells to convert it back into electricity.<sup>192</sup> Japan and other countries have detailed plans for a “H<sub>2</sub> society”, where hydrogen is a key component of their energy systems, as stated in their Strategic Energy Plans.<sup>193</sup> The “H<sub>2</sub>@Scale” vision has been introduced by scientists at the National Renewable Energy Laboratory. Various sectors, for instance industry, grid power, and transportation, incorporate H<sub>2</sub> into their operations, resulting in advantages like increased energy security.<sup>194</sup>

The concept of the H<sub>2</sub> economy is not far-fetched. Presently, gray and blue H<sub>2</sub> are priced between \$1.20 and \$2.40 per kilogram, subject to the expense of carbon capture and storage. The cost of green hydrogen is approximately \$4.85 per kilogram, taking into account an electricity cost of \$53 per MW h and an efficiency of 65% at nominal capacity based on the lower heating value. However, it is anticipated that declining renewable electricity costs, enhanced electrolyzer efficiency, and reduced capital expenses will bring the cost of green H<sub>2</sub> to below \$2.00 per kilogram by 2030, making it competitive with gray H<sub>2</sub> across various sectors, including industry.<sup>195</sup> The refining sector is projected to see a rise in demand for H<sub>2</sub> in the next decade, reaching approximately 41 million metric tons per year.<sup>196</sup> Also, the demand for methanol and ammonia is projected to experience substantial growth in the foreseeable future, driven by their usage in agriculture and their role as efficient energy carriers.<sup>197</sup>

Several critical factors determine the economic viability of green H<sub>2</sub> production plants. Firstly, it is essential to have



Table 5 Comparison of different fuel cell types, these data taken from.<sup>191</sup>

	SOFCs	MCFCs	PAFCs	AFCs	PEMFCs
Electrolyte	Ceramics	Molten carbonate	Phosphoric acid	Potassium hydroxide	Polymeric membrane
Charge carriers	O <sup>2-</sup>	CO <sub>3</sub> <sup>2-</sup>	H <sup>+</sup>	OH <sup>-</sup>	H <sup>+</sup>
Operating temperature	500 to 1000 °C	600 to 700 °C	150 to 220 °C	50 to 200 °C	-40 to 120 °C (150 to 180 °C in high temp. PEMFCs)
Electrical efficiency	Up to 65%	Up to 60%	Up to 45%	Up to 70%	Up to 65–72%
Primary fuel	H <sub>2</sub> , biogas, or methane	H <sub>2</sub> , biogas, or CH <sub>4</sub>	H <sub>2</sub> or reformed H <sub>2</sub>	H <sub>2</sub> or cracked ammonia	H <sub>2</sub> , reformed H <sub>2</sub> , methanol in direct methanol fuel cells
Primary applications	Stationary	Stationary	Stationary	Portable and stationary	Portable, transportation, and small-scale stationary
Power delivery (2019)	78.1 MW	10.2 MW	106.7 MW	0 MW	934.2 MW

a substantial H<sub>2</sub> demand to justify the investment in such facilities. The industrial sector, particularly in applications such as steel production and chemicals, presents a significant opportunity for the utilization of green H<sub>2</sub>. Moreover, the economic feasibility is further enhanced when electricity prices are low, as the energy-intensive electrolysis process relies on affordable power sources. Additionally, the presence of high carbon taxes incentivizes industries to transition towards cleaner energy sources, making green H<sub>2</sub> a cost-effective solution for reducing emissions.

However, there are numerous challenges and opportunities associated with green H<sub>2</sub> production. One of the foremost challenges is the integration of these facilities with the existing energy grid. It can be challenging to balance intermittent renewable energy sources, such as solar and wind, with the steady demand for H<sub>2</sub>. Effective grid integration and energy storage solutions are critical to address this issue. Moreover, transportation and storage of H<sub>2</sub>, whether in gaseous or liquid form, pose logistical challenges. Infrastructure development is required to facilitate the efficient distribution and utilization of green hydrogen.

Lastly, policy support is paramount for the growth of the green H<sub>2</sub> sector. Governments can incentivize investment through subsidies and regulations that promote cleaner energy sources. By addressing these challenges and capitalizing on the opportunities, green H<sub>2</sub> production can become a transformative force in promoting sustainable energy solutions and reducing carbon emissions.

## 6. Limitations and future outlooks

It's evident that green H<sub>2</sub> holds significant promise for transitioning to sustainable energy systems and substantially reducing carbon emissions. However, several challenges need to be addressed to realize its potential fully. The primary obstacle is the high production cost of green H<sub>2</sub> compared to hydrogen derived from fossil fuels, driven by the expenses associated with renewable energy sources and electrolysis technology. Additionally, the intermittent nature of renewable energy sources like wind and solar impacts the continuous availability of green H<sub>2</sub>, making grid integration and energy storage solutions crucial for a stable supply. Efficient transportation and storage of hydrogen also pose challenges,

requiring specialized infrastructure and incurring additional costs for processes like compression, liquefaction, or using chemical carriers. Furthermore, meeting the growing demand for green hydrogen through mass production is complex, necessitating the scaling up of production facilities while maintaining economic viability.

Despite these challenges, the outlook for green hydrogen integration into large-scale projects is promising, aligning with the vision for a sustainable future by 2050. Technological advancements and increased production scales are expected to lower the cost of green H<sub>2</sub>. As renewable energy becomes more competitive, the production costs of green H<sub>2</sub> will benefit from reduced energy expenses. Research and development efforts are anticipated to yield more efficient and cost-effective electrolysis technologies, with breakthroughs in catalyst materials and cell designs significantly enhancing production efficiency. Establishing hydrogen infrastructure, such as pipelines and storage solutions, will facilitate the broad adoption of green H<sub>2</sub> across various industries, including transportation and power generation. Supportive government policies, including subsidies and carbon pricing mechanisms, are increasingly recognizing the role of green H<sub>2</sub> in decarbonizing industries, encouraging investment and growth in this sector. Regions rich in renewable energy are exploring the potential for exporting green H<sub>2</sub>, creating new economic opportunities and fostering international cooperation. Industries like chemicals and steel are progressively transitioning to green H<sub>2</sub> as a cleaner feedstock, driving demand and further reducing costs through economies of scale.

## 7. Conclusion

The adaptability and environmental advantages of green hydrogen have led to increased attention in sustainable energy. Renewable sources like solar and wind energy power the electrolysis process that splits water, creating this environmentally friendly energy carrier. It represents hope in our transition to a low-carbon economy, unlike gray hydrogen, which is derived from fossil fuels and contributes to harmful emissions. Green hydrogen offers a cleaner and more sustainable alternative, supporting global efforts to fight climate change and reduce reliance on finite resources. The potential of green hydrogen lies in its ability to transform different sectors, particularly



transportation and industry. Green hydrogen offers emission-free alternatives to conventional fossil fuel vehicles, making it a practical solution for governments and industries worldwide aiming to reduce transportation emissions. By replacing diesel and oil, it helps reduce harmful emissions and promotes energy independence and resilience in transportation. Moreover, green hydrogen has applications not only in transportation but also in chemical manufacturing and heavy industry. The versatility of this raw material opens up possibilities for sustainable production through different chemical processes. Green hydrogen enables the synthesis of chemicals like ammonia, methanol, and ethanol, reducing carbon emissions and fostering innovation and competitiveness in these industries. Green hydrogen holds the potential for cost and energy reduction in steelmaking. Replacing coke and coal with hydrogen in iron reduction can greatly reduce greenhouse gas emissions, promoting sustainability in heavy industries. The rise of green hydrogen signifies a major transition to a greener, more sustainable energy future. Its significance in our joint endeavors to combat climate change and build a sustainable future for generations to come is highlighted by its ability to reduce carbon emissions in transportation, transform chemical manufacturing, and enhance the efficiency of heavy industries.

## Data availability

No new data were created or analysed during this study. Data sharing is not applicable to this article.

## Conflicts of interest

There are no conflicts to declare.

## References

- G. Kalt, *et al.*, Conceptualizing energy services: A review of energy and well-being along the Energy Service Cascade, *Energy Res. Social Sci.*, 2019, **53**, 47–58.
- A. Vahidi and A. Sciarretta, Energy saving potentials of connected and automated vehicles, *Transport. Res. C Emerg. Technol.*, 2018, **95**, 822–843.
- E. M. Oziolor, *et al.*, Adaptive introgression enables evolutionary rescue from extreme environmental pollution, *Science*, 2019, **364**(6439), 455–457.
- S. Wei, W. Jiandong and H. Saleem, The impact of renewable energy transition, green growth, green trade and green innovation on environmental quality: Evidence from top 10 green future countries, *Front. Environ. Sci.*, 2023, **10**, 1076859.
- I. Youm, *et al.*, Renewable energy activities in Senegal: a review, *Renew. Sustain. Energy Rev.*, 2000, **4**(1), 75–89.
- G. Hiemstra-van der Horst and A. J. Hovorka, Fuelwood: the “other” renewable energy source for Africa?, *Biomass Bioenergy*, 2009, **33**(11), 1605–1616.
- D. Hall, Cooling the greenhouse with bioenergy, *Nature*, 1991, **353**(6339), 11–12.
- C. Global, *Emissions in 2019–Analysis*, IEA, 2020.
- M. Child, *et al.*, Sustainability guardrails for energy scenarios of the global energy transition, *Renew. Sustain. Energy Rev.*, 2018, **91**, 321–334.
- V. M. Maestre Muñoz, A. Ortiz Sainz de Aja, and I. Ortiz Uribe, *Challenges and Prospects of Renewable Hydrogen-Based Strategies for Full Decarbonization of Stationary Power Applications*, 2021.
- T. Abbas, *et al.*, Biomass combined heat and power generation for Anticosti Island: A case study, *J. Energy Power Eng.*, 2020, **8**(03), 64.
- B. R. Kumar, Case 16: Three Gorges Dam—The World’s Largest Hydroelectric Plant, in *Project Finance: Structuring, Valuation and Risk Management for Major Projects*, Springer, 2022, p. 183–186.
- H.-Y. Wang, *et al.*, Optimal wind energy generation considering climatic variables by Deep Belief network (DBN) model based on modified coot optimization algorithm (MCOA), *Sustain. Energy Technol. Assessments*, 2022, **53**, 102744.
- M. Sutcu, *et al.*, Decision Making Of Suitable Bioenergy Power Plant Location: A Case Study. in *ICRMAT*. 2020.
- T. Simla and W. Stanek, Influence of the wind energy sector on thermal power plants in the Polish energy system, *Renewable Energy*, 2020, **161**, 928–938.
- Z. Yang, *et al.*, Sizing utility-scale photovoltaic power generation for integration into a hydropower plant considering the effects of climate change: a case study in the Longyangxia of China, *Energy*, 2021, **236**, 121519.
- S. A. Awuku, *et al.*, Promoting the Solar Industry in Ghana through Effective Public-Private Partnership (PPP): Some Lessons from South Africa and Morocco, *Energies*, 2021, **15**(1), 17.
- B. R. Kumar, Case 21: Bhadla Solar Park, in *Project Finance: Structuring, Valuation and Risk Management for Major Projects*, Springer, 2022, p. 205–208.
- K. Beladjine, F. Sadji and R. Beladjine, China Experience in Renewable Energies, *Prospects*, 2022, **60**(01), 700–718.
- I. E. Agency, *World Energy Investment 2022*, OECD Publishing, 2022.
- M. Yue, *et al.*, Hydrogen energy systems: A critical review of technologies, applications, trends and challenges, *Renew. Sustain. Energy Rev.*, 2021, **146**, 111180.
- S. Bellani, M. R. Antognazza and F. Bonaccorso, Carbon-Based Photocathode Materials for Solar Hydrogen Production, *Adv. Mater.*, 2019, **31**(9), 1801446.
- Y. Wang, *et al.*, Non-Noble Metal-Based Catalysts Applied to Hydrogen Evolution from Hydrolysis of Boron Hydrides, *Small Struct.*, 2021, **2**(7), 2000135.
- D. J. Veerendra Kumar, *et al.*, Performance evaluation of 1.1 mw grid-connected solar photovoltaic power plant in louisiana, *Energies*, 2022, **15**(9), 3420.
- D. F. Duvenhage, *et al.*, Optimising the concentrating solar power potential in South Africa through an improved GIS analysis, *Energies*, 2020, **13**(12), 3258.
- J. Marchand, *et al.*, Emt real-time simulation model of a 2 gw offshore renewable energy hub integrating electrolyzers, *Energies*, 2021, **14**(24), 8547.



- 27 Y. Himri, *et al.*, Overview of the Role of Energy Resources in Algeria's Energy Transition, *Energies*, 2022, **15**(13), 4731.
- 28 Y. Yu, *et al.*, Study on the Motion Characteristics of 10 MW Superconducting Floating Offshore Wind Turbine Considering 2nd Order Wave Effect, *Energies*, 2021, **14**(19), 6070.
- 29 Y. Baba, A. H. Pandyaswargo and H. Onoda, An analysis of the current status of woody biomass gasification power generation in Japan, *Energies*, 2020, **13**(18), 4903.
- 30 F. Battista, N. Frison and D. Bolzonella, Energy and nutrients' recovery in anaerobic digestion of agricultural biomass: An Italian perspective for future applications, *Energies*, 2019, **12**(17), 3287.
- 31 E. P. Garduño-Ruiz, *et al.*, Criteria for optimal site selection for ocean thermal energy conversion (OteC) plants in Mexico, *Energies*, 2021, **14**(8), 2121.
- 32 K.-W. Ng, W.-H. Lam and K.-C. Ng, 2002–2012: 10 Years of Research Progress in Horizontal-Axis Marine Current Turbines, *Energies*, 2013, **6**(3), 1497–1526.
- 33 V. Panchenko, *et al.*, Prospects for the production of green hydrogen: Review of countries with high potential, *Int. J. Hydrogen Energy*, 2023, **48**(12), 4551–4571.
- 34 M. A. Salam, *et al.*, A review of hydrogen production via biomass gasification and its prospect in Bangladesh, *Int. J. Hydrogen Energy*, 2018, **43**(32), 14944–14973.
- 35 A. M. Nasrabadi and M. Korpeh, Techno-economic analysis and optimization of a proposed solar-wind-driven multigeneration system; case study of Iran, *Int. J. Hydrogen Energy*, 2023, **48**(36), 13343–13361.
- 36 Y. Hu, *et al.*, Experimental evaluation of methanol steam reforming reactor heated by catalyst combustion for kW-class SOFC, *Int. J. Hydrogen Energy*, 2023, **48**(12), 4649–4664.
- 37 C. T. Rodrigues, *et al.*, An autonomous fuel cell: Methanol and dimethyl ether steam reforming direct fed to fuel cell, *Int. J. Hydrogen Energy*, 2023, **48**(10), 4052–4063.
- 38 A. V. Vorontsov and P. G. Smirniotis, Advancements in hydrogen energy research with the assistance of computational chemistry, *Int. J. Hydrogen Energy*, 2023, 14978–14999.
- 39 W. Zhou, *et al.*, Energy-saving cathodic H<sub>2</sub> production enabled by non-oxygen evolution anodic reactions: a critical review on fundamental principles and applications, *Int. J. Hydrogen Energy*, 2023, 15748–15770.
- 40 X. Ren, *et al.*, Challenges towards hydrogen economy in China, *Int. J. Hydrogen Energy*, 2020, **45**(59), 34326–34345.
- 41 M. S. Ahmad, M. S. Ali and N. Abd Rahim, Hydrogen energy vision 2060: Hydrogen as energy carrier in Malaysian primary energy mix—Developing P2G case, *Energy Strategy Rev.*, 2021, **35**, 100632.
- 42 P. Colbertaldo, *et al.*, Impact of hydrogen energy storage on California electric power system: Towards 100% renewable electricity, *Int. J. Hydrogen Energy*, 2019, **44**(19), 9558–9576.
- 43 H. Zhang, *et al.*, Material challenges in green hydrogen ecosystem, *Coord. Chem. Rev.*, 2023, **494**, 215272.
- 44 M.-N. N. Shafiqah, *et al.*, Advanced catalysts and effect of operating parameters in ethanol dry reforming for hydrogen generation. A review, *Environ. Chem. Lett.*, 2022, **20**(3), 1695–1718.
- 45 C. Park, *et al.*, Economic valuation of green hydrogen charging compared to gray hydrogen charging: The case of South Korea, *Int. J. Hydrogen Energy*, 2022, **47**(32), 14393–14403.
- 46 M. Hirscher, *et al.*, Materials for hydrogen-based energy storage – past, recent progress and future outlook, *J. Alloys Compd.*, 2020, **827**, 153548.
- 47 F. Qureshi, *et al.*, Current trends in hydrogen production, storage and applications in India: A review, *Sustain. Energy Technol. Assessments*, 2022, **53**, 102677.
- 48 T. Liu, K. Yang and Z. Jin, Promotion of the excited electron transfer over MoO<sub>3</sub>@Cu<sub>3</sub>P p–n heterojunction for photocatalytic hydrogen production under visible light irradiation, *Mol. Catal.*, 2021, **510**, 111691.
- 49 T. Van de Graaf, *et al.*, The new oil? The geopolitics and international governance of hydrogen, *Energy Res. Social Sci.*, 2020, **70**, 101667.
- 50 M. Noussan, *et al.*, The role of green and blue hydrogen in the energy transition—A technological and geopolitical perspective, *Sustainability*, 2021, **13**(1), 298.
- 51 J. Lin, *et al.*, Phyto-mediated synthesis of nanoparticles and their applications on hydrogen generation on NaBH<sub>4</sub>, biological activities and photodegradation on azo dyes: Development of machine learning model, *Food Chem. Toxicol.*, 2022, **163**, 112972.
- 52 A. N. Antzaras and A. A. Lemonidou, Recent advances on materials and processes for intensified production of blue hydrogen, *Renew. Sustain. Energy Rev.*, 2022, **155**, 111917.
- 53 C. Bauer, *et al.*, On the climate impacts of blue hydrogen production, *Sustain. Energy Fuels*, 2022, **6**(1), 66–75.
- 54 W. Su, *et al.*, Hydrogen production and heavy metal immobilization using hyperaccumulators in supercritical water gasification, *J. Hazard. Mater.*, 2021, **402**, 123541.
- 55 W. Su, *et al.*, Supercritical water gasification of hyperaccumulators for hydrogen production and heavy metal immobilization with alkali metal catalysts, *Environ. Res.*, 2022, **214**, 114093.
- 56 S. Atilhan, *et al.*, Green hydrogen as an alternative fuel for the shipping industry, *Curr. Opin. Chem. Eng.*, 2021, **31**, 100668.
- 57 R. d'Amore-Domenech, Ó. Santiago and T. J. Leo, Multicriteria analysis of seawater electrolysis technologies for green hydrogen production at sea, *Renew. Sustain. Energy Rev.*, 2020, **133**, 110166.
- 58 E. R. Sadik-Zada, Political Economy of Green Hydrogen Rollout: A Global Perspective, *Sustainability*, 2021, **13**(23), 13464.
- 59 Z. Xu, *et al.*, High temperature hydrothermal etching of g-C<sub>3</sub>N<sub>4</sub> for synthesis of N doped carbon quantum dots-supported CdS photocatalyst to enhance visible light driven hydrogen generation, *Mol. Catal.*, 2022, **517**, 111900.
- 60 H. Zhao, *et al.*, Raw biomass electroreforming coupled to green hydrogen generation, *Nat. Commun.*, 2021, **12**(1), 2008.



- 61 R. Rahimpour and A. Basile, *Special Issue "Novel Catalysts Development for Hydrogen Production"*, Elsevier, 2023, p. 6157.
- 62 A. Inayat, *et al.*, A comprehensive review on advanced thermochemical processes for bio-hydrogen production via microwave and plasma technologies, *Biomass Convers. Biorefin.*, 2020, 1–10.
- 63 S. Balusamy, *Development of Biofuel from Nigella Sativa Biomass and its Suitability for Energy Application*, 2020.
- 64 D. Mohan, C. U. Pittman Jr and P. H. Steele, Pyrolysis of wood/biomass for bio-oil: a critical review, *Energy Fuel.*, 2006, **20**(3), 848–889.
- 65 M. Danthurebandara, *et al.*, Environmental and economic performance of plasma gasification in Enhanced Landfill Mining, *Waste Manage.*, 2015, **45**, 458–467.
- 66 V. Zhovtyansky and V. Valinčius, Efficiency of plasma gasification technologies for hazardous waste treatment, *Gasification for Low-Grade Feedstock*, 2018, p. 165–189.
- 67 M. Hlina, *et al.*, Plasma gasification of wood and production of gas with low content of tar, *Czech J. Phys.*, 2006, **56**, B1179–B1184.
- 68 M. Jasiński, *et al.*, Hydrogen production via methane reforming using various microwave plasma sources, *Chem. Listy*, 2008, **102**(16), S1332–S1337.
- 69 C. M. Kalamaras and A. M. Efstathiou. Hydrogen production technologies: current state and future developments, in *Conference papers in science*, Hindawi, 2013.
- 70 C. Du, J. Mo and H. Li, Renewable hydrogen production by alcohols reforming using plasma and plasma-catalytic technologies: challenges and opportunities, *Chem. Rev.*, 2015, **115**(3), 1503–1542.
- 71 S. A. Bhat and J. Sadhukhan, Process intensification aspects for steam methane reforming: An overview, *AIChE J.*, 2009, **55**(2), 408–422.
- 72 M. Balat and E. Kirtay, Major technical barriers to a "hydrogen economy", *Energy Sources, Part A*, 2010, **32**(9), 863–876.
- 73 G. W. Crabtree, M. S. Dresselhaus and M. V. Buchanan, The hydrogen economy, *Phys. Today*, 2004, **57**(12), 39–44.
- 74 G. W. Crabtree and M. S. Dresselhaus, The hydrogen fuel alternative, *MRS Bull.*, 2008, **33**(4), 421–428.
- 75 P.-C. Kuo, *et al.*, Plasma gasification performances of various raw and torrefied biomass materials using different gasifying agents, *Bioresour. Technol.*, 2020, **314**, 123740.
- 76 A. A. Haleem, *et al.*, A new accelerated durability test protocol for water oxidation electrocatalysts of renewable energy powered alkaline water electrolyzers, *Electrochemistry*, 2021, **89**(2), 186–191.
- 77 G. Petipas, *et al.*, A comparative study of non-thermal plasma assisted reforming technologies, *Int. J. Hydrogen Energy*, 2007, **32**(14), 2848–2867.
- 78 J. Makavana, *et al.*, Development and performance evaluation of batch type biomass pyrolyser for agricultural residue, *Biomass Convers. Biorefin.*, 2020, 1–8.
- 79 S. Pang, Advances in thermochemical conversion of woody biomass to energy, fuels and chemicals, *Biotechnol. Adv.*, 2019, **37**(4), 589–597.
- 80 M. Saidi, M. H. Gohari and A. T. Ramezani, Hydrogen production from waste gasification followed by membrane filtration: a review, *Environ. Chem. Lett.*, 2020, **18**, 1529–1556.
- 81 T. Wu, *et al.*, Plasma bubble characteristics and hydrogen production performance of methanol decomposition by liquid phase discharge, *Energy*, 2023, **273**, 127252.
- 82 B. Tabu, *et al.*, Nonthermal atmospheric plasma reactors for hydrogen production from low-density polyethylene, *Int. J. Hydrogen Energy*, 2022, **47**(94), 39743–39757.
- 83 Y. Zhang, *et al.*, Simultaneously efficient solar light harvesting and charge transfer of hollow octahedral Cu<sub>2</sub>S/CdS p–n heterostructures for remarkable photocatalytic hydrogen generation, *Trans. Tianjin Univ.*, 2021, **27**(4), 348–357.
- 84 Y. Tian, *et al.*, Thiophene-Conjugated Porous C<sub>3</sub>N<sub>4</sub> Nanosheets for Boosted Photocatalytic Nicotinamide Cofactor Regeneration to Facilitate Solar-to-Chemical Enzymatic Reactions, *Trans. Tianjin Univ.*, 2021, **27**(1), 42–54.
- 85 R. G. Lemus and J. M. M. Duarte, Updated hydrogen production costs and parities for conventional and renewable technologies, *Int. J. Hydrogen Energy*, 2010, **35**(9), 3929–3936.
- 86 A. Ursúa, *et al.*, Integration of commercial alkaline water electrolyzers with renewable energies: Limitations and improvements, *Int. J. Hydrogen Energy*, 2016, **41**(30), 12852–12861.
- 87 L. M. Gandía, *et al.*, Renewable hydrogen production: performance of an alkaline water electrolyzer working under emulated wind conditions, *Energy Fuel.*, 2007, **21**(3), 1699–1706.
- 88 A. Ursúa, *et al.*, Stand-alone operation of an alkaline water electrolyser fed by wind and photovoltaic systems, *Int. J. Hydrogen Energy*, 2013, **38**(35), 14952–14967.
- 89 J. M. Stansberry and J. Brouwer, Experimental dynamic dispatch of a 60 kW proton exchange membrane electrolyzer in power-to-gas application, *Int. J. Hydrogen Energy*, 2020, **45**(16), 9305–9316.
- 90 H. Zhang, H. Wang and J. Xuan, Rational design of photoelectrochemical cells towards bias-free water splitting: Thermodynamic and kinetic insights, *J. Power Sources*, 2020, **462**, 228113.
- 91 D. Zheng, *et al.*, Nanocatalysts in photocatalytic water splitting for green hydrogen generation: Challenges and opportunities, *J. Cleaner Prod.*, 2023, **414**, 137700.
- 92 X. Yan, *et al.*, An electron-hole rich dual-site nickel catalyst for efficient photocatalytic overall water splitting, *Nat. Commun.*, 2023, **14**(1), 1741.
- 93 J. Ruan, T. Zhong and Y. Guo, Enhanced water splitting over ethylenediaminetetraacetate treated SrTiO<sub>3</sub> photocatalysts with high crystallinity, reduced size, and surface nanostructure, *J. Colloid Interface Sci.*, 2023, **650**, 1424–1433.



- 94 M. Saleh, *et al.*, Enhancing photocatalytic water splitting: Comparative study of TiO<sub>2</sub> decorated nanocrystals (Pt and Cu) using different synthesis methods, *Fuel*, 2023, **354**, 129248.
- 95 Q. Lai, *et al.*, Hydrogen storage materials for mobile and stationary applications: current state of the art, *ChemSusChem*, 2015, **8**(17), 2789–2825.
- 96 Y. Zhang, *et al.*, Solidified Hydrogen Storage (Solid-HyStore) via Clathrate Hydrates, *Chem. Eng. J.*, 2022, **431**, 133702.
- 97 Z. Zhang, *et al.*, Heterostructured VF<sub>4</sub>@Ti<sub>3</sub>C<sub>2</sub> catalyst improving reversible hydrogen storage properties of Mg(BH<sub>4</sub>)<sub>2</sub>, *Chem. Eng. J.*, 2023, **460**, 141690.
- 98 J. Liu, *et al.*, High performance stainless-steel supported Pd membranes with a finger-like and gap structure and its application in NH<sub>3</sub> decomposition membrane reactor, *Chem. Eng. J.*, 2020, **388**, 124245.
- 99 V. Nicolas, *et al.*, Numerical simulation of a thermally driven hydrogen compressor as a performance optimization tool, *Appl. Energy*, 2022, **323**, 119628.
- 100 H. Nazir, *et al.*, Is the H<sub>2</sub> economy realizable in the foreseeable future? Part II: H<sub>2</sub> storage, transportation, and distribution, *Int. J. Hydrogen Energy*, 2020, **45**(41), 20693–20708.
- 101 A. Goepfert, *et al.*, Recycling of carbon dioxide to methanol and derived products-closing the loop, *Chem. Soc. Rev.*, 2014, **43**(23), 7995–8048.
- 102 Y. Shen, *et al.*, Hydrogen generation from methanol at near-room temperature, *Chem. Sci.*, 2017, **8**(11), 7498–7504.
- 103 M. Bui, *et al.*, Carbon capture and storage (CCS): the way forward, *Energy Environ. Sci.*, 2018, **11**(5), 1062–1176.
- 104 S. Enthaler, J. von Langermann and T. Schmidt, Carbon dioxide and formic acid—the couple for environmental-friendly hydrogen storage?, *Energy Environ. Sci.*, 2010, **3**(9), 1207–1217.
- 105 D. A. Bulushev and J. R. Ross, Towards sustainable production of formic acid, *ChemSusChem*, 2018, **11**(5), 821–836.
- 106 K. C. Ott, *Final Report for the DOE Chemical Hydrogen Storage Center of Excellence*, Los Alamos National Laboratory, 2012.
- 107 X. Yang, *et al.*, Stable electrolysis of ammonia on platinum enhanced by methanol in non-aqueous electrolyte for an in-situ hydrogen production, *Chem. Eng. J.*, 2022, **442**, 136167.
- 108 M. Aziz, A. T. Wijayanta and A. B. D. Nandiyanto, Ammonia as Effective Hydrogen Storage: A Review on Production, Storage and Utilization, *Energies*, 2020, **13**(12), 3062.
- 109 K. E. Lamb, M. D. Dolan and D. F. Kennedy, Ammonia for hydrogen storage; A review of catalytic ammonia decomposition and hydrogen separation and purification, *Int. J. Hydrogen Energy*, 2019, **44**(7), 3580–3593.
- 110 F. Schüth, *et al.*, Ammonia as a possible element in an energy infrastructure: Catalysts for ammonia decomposition, *Energy Environ. Sci.*, 2012, **5**(4), 6278–6289.
- 111 A. Klerke, *et al.*, Ammonia for hydrogen storage: challenges and opportunities, *J. Mater. Chem.*, 2008, **18**(20), 2304–2310.
- 112 D. Lim, *et al.*, Life cycle techno-economic and carbon footprint analysis of H<sub>2</sub> production via NH<sub>3</sub> decomposition: A Case study for the Republic of Korea, *Energy Convers. Manage.*, 2021, **250**, 114881.
- 113 F. Jiao and B. Xu, Electrochemical Ammonia Synthesis and Ammonia Fuel Cells, *Adv. Mater.*, 2019, **31**(31), 1805173.
- 114 S. Ramalingam, M. DhakshinaMoorthy and S. Subramanian, Effect of natural antioxidant additive on hydrogen-enriched biodiesel operated compression ignition engine, *Int. J. Hydrogen Energy*, 2022, **47**(48), 20771–20783.
- 115 B. P. Tarasov, *et al.*, Metal hydride–Graphene composites for hydrogen based energy storage, *J. Alloys Compd.*, 2022, **896**, 162881.
- 116 A. W. van den Berg and C. O. Areán, Materials for hydrogen storage: current research trends and perspectives, *Chem. Commun.*, 2008, (6), 668–681.
- 117 G. Sandrock, A panoramic overview of hydrogen storage alloys from a gas reaction point of view, *J. Alloys Compd.*, 1999, **293–295**, 877–888.
- 118 Y. Liu, *et al.*, Nanostructured light metal hydride: Fabrication strategies and hydrogen storage performance, *Renew. Sustain. Energy Rev.*, 2023, **184**, 113560.
- 119 S. Weitemeyer, *et al.*, Integration of Renewable Energy Sources in future power systems: The role of storage, *Renewable Energy*, 2015, **75**, 14–20.
- 120 M. V. Lototskyy, *et al.*, Metal hydride hydrogen compressors: A review, *Int. J. Hydrogen Energy*, 2014, **39**(11), 5818–5851.
- 121 A. V. Rusanov, V. V. Solovey and M. V. Lototskyy, Thermodynamic features of metal hydride thermal sorption compressors and perspectives of their application in hydrogen liquefaction systems, *J. Phys. Energy*, 2020, **2**, 021007.
- 122 M. Song, *et al.*, Recent advances of magnesium hydride as an energy storage material, *J. Mater. Sci. Technol.*, 2023, **149**, 99–111.
- 123 P. Thongtan, *et al.*, MgH<sub>2</sub>-based hydrogen storage tank: Kinetics, reversibility, and MWCNTs content, *J. Phys. Chem. Solids*, 2022, **163**, 110578.
- 124 H. Gao, *et al.*, Solid-solution MAX phase TiVAIC assisted with impurity for enhancing hydrogen storage performance of magnesium hydride, *J. Colloid Interface Sci.*, 2023, **652**, 979–988.
- 125 S. Li, *et al.*, Enhanced hydrogen storage performance of magnesium hydride catalyzed by medium-entropy alloy CrCoNi nanosheets, *Int. J. Hydrogen Energy*, 2023.
- 126 L. Zhang, *et al.*, Carbon-wrapped Ti-Co bimetallic oxide nanocages: Novel and efficient catalysts for hydrogen storage in magnesium hydride, *J. Alloys Compd.*, 2023, **952**, 170002.
- 127 R. Jiang, *et al.*, Remarkable hydrogen absorption/desorption behaviors and mechanism of sodium alanates in-situ doped with Ti-based 2D MXene, *Mater. Chem. Phys.*, 2020, **242**, 122529.



- 128 N. A. Ali and M. Ismail, Modification of NaAlH<sub>4</sub> properties using catalysts for solid-state hydrogen storage: A review, *Int. J. Hydrogen Energy*, 2021, **46**(1), 766–782.
- 129 N. A. Ali, *et al.*, Enhanced hydrogen storage properties of NaAlH<sub>4</sub> with the addition of CoTiO<sub>3</sub> synthesised via a solid-state method, *J. Alloys Compd.*, 2023, **934**, 167932.
- 130 A.-b. H. Mekky, Electronic structure and stability of a pure sodium alanate clusters Na<sub>12</sub>Al<sub>12</sub>H<sub>48</sub>, and the interstitial space-doped with Ti, C and H atoms, as a promising hydrogen storage system: Density functional theory, *Int. J. Hydrogen Energy*, 2023, **48**(53), 20430–20440.
- 131 R. U. Urunkar and S. D. Patil, Performance analysis of sodium alanate hydride reactor with different nanofluids, *Int. J. Hydrogen Energy*, 2023.
- 132 E. Taibi, *et al.*, *Hydrogen from Renewable Power: Technology Outlook for the Energy Transition*, 2018.
- 133 R. Shinnar, The hydrogen economy, fuel cells, and electric cars, *Technol. Soc.*, 2003, **25**(4), 455–476.
- 134 M. Kong, *et al.*, Investigation of Mixing Behavior of Hydrogen Blended to Natural Gas in Gas Network, *Sustainability*, 2021, **13**(8), 4255.
- 135 R. D. F.-G. Gaz, *et al.*, *Technical and Economic Conditions for Injecting Hydrogen into Natural Gas Networks-Final Report June 2019*, 2019.
- 136 A. G. Australia, *Clean energy Innovation Hub lessons. Arena Insights Forum 2019: 2e8*, 2019.
- 137 T. Isaac, HyDeploy: The UK's first hydrogen blending deployment project, *Clean Energy*, 2019, **3**(2), 114–125.
- 138 B. Neal, *et al.*, Rationale, design and baseline characteristics of the CANagliflozin cardiovascular Assessment Study–Renal (CANVAS-R): A randomized, placebo-controlled trial, *Diabetes Obes. Metabol.*, 2017, **19**(3), 387–393.
- 139 Y. Zhao, V. McDonnell and S. Samuelsen, Influence of hydrogen addition to pipeline natural gas on the combustion performance of a cooktop burner, *Int. J. Hydrogen Energy*, 2019, **44**(23), 12239–12253.
- 140 D. Krieg, *Konzept und Kosten eines Pipelinesystems zur Versorgung des deutschen Straßenverkehrs mit Wasserstoff*, 2012, Forschungszentrum Jülich, vol. 144.
- 141 M. Ozturk, *et al.*, An experimental study on the environmental impact of hydrogen and natural gas blend burning, *Chemosphere*, 2023, **329**, 138671.
- 142 M. Ozturk and I. Dincer, System development and assessment for green hydrogen generation and blending with natural gas, *Energy*, 2022, **261**, 125233.
- 143 D. Kushnir, *et al.*, Adopting hydrogen direct reduction for the Swedish steel industry: A technological innovation system (TIS) study, *J. Cleaner Prod.*, 2020, **242**, 118185.
- 144 A. Hasanbeigi, M. Arens and L. Price, Alternative emerging ironmaking technologies for energy-efficiency and carbon dioxide emissions reduction: A technical review, *Renew. Sustain. Energy Rev.*, 2014, **33**, 645–658.
- 145 X. Tan, *et al.*, Energy-saving and emission-reduction technology selection and CO<sub>2</sub> emission reduction potential of China's iron and steel industry under energy substitution policy, *J. Cleaner Prod.*, 2019, **222**, 823–834.
- 146 Z.-j. Liu, J.-l. Zhang and T.-j. Yang, Low Carbon Operation of Super-Large Blast Furnaces in China, *ISIJ Int.*, 2015, **55**(6), 1146–1156.
- 147 D. Spreitzer and J. Schenk, Reduction of iron oxides with hydrogen—a review, *Steel Res. Int.*, 2019, **90**(10), 1900108.
- 148 S. Zheng, Basic research on hydrogen metallurgy and new ironmaking idea-process, *China Metall.*, 2012, **22**, 1–6.
- 149 G. Wang, *et al.*, Effect of blast furnace gas recycling with hydrogen injection on low carbon development of Chinese ironmaking, *Metall.*, 2019, **29**(10), 1.
- 150 K. Cao, *et al.*, H<sub>2</sub>-rich reduction kinetics of iron ore sinter, *Chin. J. Process Eng.*, 2015, **15**(6), 1024–1028.
- 151 M.-H. Bai, *et al.*, Reduction behavior and kinetics of iron ore pellets under H<sub>2</sub>-N<sub>2</sub> atmosphere, *ISIJ Int.*, 2018, **58**(6), 1034–1041.
- 152 Y. Man and J. Feng, Effect of gas composition on reduction behavior in red mud and iron ore pellets, *Powder Technol.*, 2016, **301**, 674–678.
- 153 Q. Lyu, *et al.*, Effect of hydrogen addition on reduction behavior of iron oxides in gas-injection blast furnace, *Thermochim. Acta*, 2017, **648**, 79–90.
- 154 S. K. Kuila, R. Chatterjee and D. Ghosh, Kinetics of hydrogen reduction of magnetite ore fines, *Int. J. Hydrogen Energy*, 2016, **41**(22), 9256–9266.
- 155 D. Spreitzer and J. Schenk, Iron ore reduction by hydrogen using a laboratory scale fluidized bed reactor: Kinetic investigation—Experimental setup and method for determination, *Metall. Mater. Trans. B*, 2019, **50**, 2471–2484.
- 156 J. Chen, S. Yang and Y. Qian, A novel path for carbon-rich resource utilization with lower emission and higher efficiency: An integrated process of coal gasification and coking to methanol production, *Energy*, 2019, **177**, 304–318.
- 157 D. Xiang, *et al.*, Techno-economic analysis of the coal-to-olefins process in comparison with the oil-to-olefins process, *Appl. Energy*, 2014, **113**, 639–647.
- 158 Q. Chen, *et al.*, Feasibility analysis of nuclear-coal hybrid energy systems from the perspective of low-carbon development, *Appl. Energy*, 2015, **158**, 619–630.
- 159 D. Xiang, *et al.*, Highly efficient carbon utilization of coal-to-methanol process integrated with chemical looping hydrogen and air separation technology: Process modeling and parameter optimization, *J. Cleaner Prod.*, 2020, **258**, 120910.
- 160 Y. Jin, Y. Zhou and S. Hu, Discussion on development of coal chemical industry using low-carbon concept, *Huagong Xuebao/CIESC J.*, 2012, **63**(1), 3–8.
- 161 X. Tang, B. Zhang, X. Wei and M. Höök, Employment impacts of petroleum industry in China: an input-output analysis, *Int. J. Global Energy Issues*, 2013, **36**(2–4), 116–129.
- 162 G. Leonzio, Methanol Synthesis: Optimal Solution for a Better Efficiency of the Process, *Processes*, 2018, **6**(3), 20.
- 163 G. A. Olah, A. Goepfert and G. K. S. Prakash, Chemical Recycling of Carbon Dioxide to Methanol and Dimethyl Ether: From Greenhouse Gas to Renewable, Environmentally Carbon Neutral Fuels and Synthetic Hydrocarbons, *J. Org. Chem.*, 2009, **74**(2), 487–498.



- 164 M. Kauw, R. M. J. Benders and C. Visser, Green methanol from hydrogen and carbon dioxide using geothermal energy and/or hydropower in Iceland or excess renewable electricity in Germany, *Energy*, 2015, **90**, 208–217.
- 165 W. Dongliang, *et al.*, Green hydrogen coupling with CO<sub>2</sub> utilization of coal-to-methanol for high methanol productivity and low CO<sub>2</sub> emission, *Energy*, 2021, **231**, 120970.
- 166 S. Sollai, *et al.*, Renewable methanol production from green hydrogen and captured CO<sub>2</sub>: A techno-economic assessment, *J. CO<sub>2</sub> Util.*, 2023, **68**, 102345.
- 167 M. Hocking, Ammonia, nitric acid and their derivatives, in *Modern Chemical Technology and Emission Control*, Springer, 1985, p. 205–233.
- 168 D. R. MacFarlane, *et al.*, A roadmap to the ammonia economy, *Joule*, 2020, **4**(6), 1186–1205.
- 169 P. Dange, *et al.*, Recent developments in microbial electrolysis cell-based biohydrogen production utilizing wastewater as a feedstock, *Sustainability*, 2021, **13**(16), 8796.
- 170 S. Kubicek and O. Spadiut, semi-artificial photosynthesis for green hydrogen production—overview, challenges and possibilities, *Symposium Energieinnovation, 16.-18.02.2022*, Graz, Austria, 2022.
- 171 S. Dahiya, *et al.*, Renewable hydrogen production by dark-fermentation: Current status, challenges and perspectives, *Bioresour. Technol.*, 2021, **321**, 124354.
- 172 S. Anwar, *et al.*, Recent development in electrocatalysts for hydrogen production through water electrolysis, *Int. J. Hydrogen Energy*, 2021, **46**(63), 32284–32317.
- 173 G. Chehade and I. Dincer, Progress in green ammonia production as potential carbon-free fuel, *Fuel*, 2021, **299**, 120845.
- 174 H. Zhao, L. M. Kamp and Z. Lukszo, The potential of green ammonia production to reduce renewable power curtailment and encourage the energy transition in China, *Int. J. Hydrogen Energy*, 2022, **47**(44), 18935–18954.
- 175 H. Ishaq, M. F. Shehzad and C. Crawford, Transient modeling of a green ammonia production system to support sustainable development, *Int. J. Hydrogen Energy*, 2023.
- 176 H. Bouaboula, *et al.*, Addressing sustainable energy intermittence for green ammonia production, *Energy Rep.*, 2023, **9**, 4507–4517.
- 177 A. Nemmour, *et al.*, Green hydrogen-based E-fuels (E-methane, E-methanol, E-ammonia) to support clean energy transition: A literature review, *Int. J. Hydrogen Energy*, 2023, **48**(75), 29011–29033.
- 178 L. Guerra, *et al.*, Methane production by a combined Sabatier reaction/water electrolysis process, *J. Environ. Chem. Eng.*, 2018, **6**(1), 671–676.
- 179 V. Pignataro, *et al.*, Impact of management strategy on green methane production from wind energy, *E3S Web Conf.*, 2023, **414**, 01005.
- 180 S. García-Luna and C. Ortiz, Conceptual assessment of sustainable methane production from oxycombustion CO<sub>2</sub> capture in waste-to-energy power plants, *Energy Convers. Manage.*, 2023, **292**, 117348.
- 181 J. Chao and B. J. Zwolinski, Ideal gas thermodynamic properties of methanoic and ethanoic acids, *J. Phys. Chem. Ref. Data*, 1978, **7**(1), 363–377.
- 182 M. E. M. Berger, *et al.*, Simple and recyclable ionic liquid based system for the selective decomposition of formic acid to hydrogen and carbon dioxide, *Green Chem.*, 2011, **13**(6), 1411–1415.
- 183 J. Hietala, *et al.*, Formic acid, *Ullmann's encyclopedia of industrial chemistry*, 2016, **1**, p. 1–22.
- 184 L. Gong, *et al.*, Power management and system optimization for high efficiency self-powered electrolytic hydrogen and formic acid production, *Nano Energy*, 2023, **107**, 108124.
- 185 J. M. Thomas, *et al.*, Decarbonising energy: The developing international activity in hydrogen technologies and fuel cells, *J. Energy Chem.*, 2020, **51**, 405–415.
- 186 L. Fan, Z. Tu and S. H. Chan, Recent development of hydrogen and fuel cell technologies: A review, *Energy Rep.*, 2021, **7**, 8421–8446.
- 187 B. Paul and J. Andrews, PEM unitised reversible/regenerative hydrogen fuel cell systems: State of the art and technical challenges, *Renew. Sustain. Energy Rev.*, 2017, **79**, 585–599.
- 188 M. C. Argyrou, P. Christodoulides and S. A. Kalogirou, Energy storage for electricity generation and related processes: Technologies appraisal and grid scale applications, *Renew. Sustain. Energy Rev.*, 2018, **94**, 804–821.
- 189 U. K. Zore, *et al.*, A review on recent advances in hydrogen energy, fuel cell, biofuel and fuel refining via ultrasound process intensification, *Ultrason. Sonochem.*, 2021, **73**, 105536.
- 190 M. F. Orhan and B. S. Babu, Investigation of an integrated hydrogen production system based on nuclear and renewable energy sources: Comparative evaluation of hydrogen production options with a regenerative fuel cell system, *Energy*, 2015, **88**, 801–820.
- 191 Y. Yu, *et al.*, Comparison of degradation behaviors for open-ended and closed proton exchange membrane fuel cells during startup and shutdown cycles, *J. Power Sources*, 2011, **196**(11), 5077–5083.
- 192 J. O. M. Bockris, A Hydrogen Economy, *Science*, 1972, **176**(4041), 1323.
- 193 M. D. Conrad and J. E. Ness, *Commonwealth of the Northern Mariana Islands Strategic Energy Plan*, National Renewable Energy Lab.(NREL), Golden, CO (United States), 2013.
- 194 B. Pivovar, N. Rustagi and S. Satyapal, Hydrogen at Scale (H<sub>2</sub>@Scale): Key to a Clean, Economic, and Sustainable Energy System, *Electrochem. Soc. Interfac.*, 2018, **27**(1), 47.
- 195 I. Irena, *Green Hydrogen Cost Reduction: Scaling up Electrolysers to Meet the 1.5 C Climate Goal*. Abu Dhabi: International Renewable Energy Agency, 2020.
- 196 I. E. Agency, *The Future of Hydrogen*. 2019.
- 197 H. Council, *Hydrogen Scaling up: a Sustainable Pathway for the Global Energy Transition*. 2017.

